Doctoral thesis

Establishment of *TSH*β real-time monitoring system in mammalian photoperiodism

Kaori Tsujino

Department of Biology
Graduate School of Science
Osaka University

Augst 2014

Abbreviations

AANAT	arylalkylamine N-acetyltransferase
AC	adenylate cyclase
AMPA	alpha-amino-3-hydroxy-5-methyl-4-isoxazolepropionic acid
cAMP	cyclic AMP
BAC	bacterial artificial chromosome
CDS	coding sequence
D	dark period
DMSO	dimethylsulfoxide
DT-A	diphtheria toxin fragment A
EC	ependymal cell layer
EM-CCD	electron-multiplying charge-coupled device
Epac	exchange protein directly activated by cAMP
Epac ag	exchange protein directly activated by cAMP agonist, 8-pCPT-2′-*O*-Me-cAMP in this study
Fsk	forskolin
Gln	glutamine
Glu	glutamic acid
GnRH	gonadotropin releasing hormone
GPCR	G-protein coupled receptors
HIOMT	hydroxyindole-*O*-methyltransferase
HPT	hypothalamus–pituitary–thyroid
IVF	*in vitro* fertilization
KA	kainic acid
L	light period
LC-SRM/MS	liquid chormatography-selected reaction monitoring/mass spectrometry
LD	long day
Luc	luciferase
MDL	MDL-12,330A (MDL), a potent, irreversible inhibitor of AC
ME	median eminence
Mel	melatonin
MT1	melatonin receptor 1A

MT2	melatonin receptor 1B
ND	not detected
NMDA	N-methyl-D-aspartic acid
NK cells	natural killer cells
PD	pars distalis
PKA	protein kinase A
PKA ag	protein kinase A agonist, 6-Bnz-cAMP in this study
PKC	protein kinase C
PLC	phospolipase C
PMT	photomultiplier tube
PT	pars tuberalis
PTX	pertussis toxin
qPCR	quantitative RT-PCR
RI	radioisotope
SCN	suprachiasmatic nucleus
SD	short day
SEM	standard error of the mean
SRM	selected reaction monitoring
SSRI	selective serotonin reuptake inhibitor
T3	triiodothyroine
T4	prohormone thyroxine
TH	thyroid hormone
TPA	12-*O*-tetradecanoyl phorbol 13-acetate (TPA), a PKC activator
TRH	thyroid releasing hormone
TSH	thyroid-stimulating hormone
TSHR	thyroid-stimulating hormone receptor
Veh	vehicle
ZT	zeitgeber time (ZT0; ZT0 was defined as the time of light-on)

Genotype representations

WT	wild-type *TSH*β^{Luc} mice
+/L	heterozygous *TSH*β^{Luc} mice
L/L	homozygous *TSH*β^{Luc} mice

Contents

Abstract

Organisms have seasonal physiological changes in response to day length. Long-day stimulation induces thyroid-stimulating hormone beta subunit (*TSH*β) in the pars tuberalis (PT), which mediates photoperiodic reactions such as day-length measurement and physiological adaptation. However, the mechanism of *TSH*β induction under the long-day condition is largely unknown. To screen candidate upstream molecules of *TSH*β, which possibly convey light information to the PT, I generated knock-in mice in which the *Luciferase* gene is targeted into the *TSH*β locus so as to quantitatively monitor the dynamics of *TSH*β expression. I cultured brain slices containing the PT region from adult and neonatal mice and measured the bioluminescence activities from each slice over several days. After the treatment of melatonin, a reported negative regulator of *TSH*β, a decrease in the bioluminescence activities were observed. These observations indicate that the slice possess *in vivo*-like responsiveness of the *TSH*β expression to melatonin. Thus, I concluded that my experimental system could monitor *TSH*β expression dynamics in response to external stimuli. I performed preliminary screening for candidate upstream molecules of *TSH*β, and I tested drugs targeting the intracellular signaling pathways, hormones, and so on, by using this monitoring system. Glutamic acid increased the bioluminescence activities acutely and transiently, consistent with previous study (Aizawa *et al.* 2012). These findings suggest that glutamic acid is a strong candidate of *TSH*β upstream molecules and this monitoring system can response to candidate *TSH*β-inducible signals. Therefore, *TSH*β real-time monitoring system is a powerful tool to screen upstream molecules of *TSH*β.

General introduction

1. General view of photoperiodism

Photoperiodism

The earth's rotation creates the daily cycle of light and darkness, while the earth's revolution with its spin axis tilted at 23.4° creates the variation in seasons. The environment varies considerably throughout the seasons, such as low food availability during winter. Organisms living in seasonal environments predict seasonal changes and adapt their physiology and behavior to promote survival. Plants flower at a specific season. Animals adapt timing of reproductive activity to produce offspring at an optimal time of year when food supply should be plentiful, while animals migrate or hibernate when food availability is low. Thus, precise timing of physiology and behavior is critical for individual reproductive success and subsequent fitness. Day-length (photoperiod) is a highly reliable cue as a calendar. Seasonal changes in day-length are constant throughout each year. Organisms can use this signal to anticipate and prepare for seasonal changes. The response of organisms to changes in day-length is known as photoperiodism, and seasonal reproduction is an example of photoperiodic responses.

Involvement of the circadian clock in photoperiodism

The circadian clock is an autonomous system that controls many physiological and behavioral systems to adapt 24-h environmental light/dark cycle. This has approximately 24-h rhythmicity in constant condition and it entrains to an exact 24-h rhythmicity by daily light. The circadian clock is composed of genes (circadian clock genes) that interact in oscillatory transcriptional networks within cells (Albrecht 2002; Ueda *et al.* 2005) and regulate the expression of many other genes critical for physiology and metabolism. The suprachiasmatic nucleus (SCN) in the hypothalamus is the master organ of the circadian clock and the SCN synchronizes all the circadian clocks in the body in mammals (Welsh *et al.* 2010).

Bünning proposed the idea that the measurement of day-length might be based on circadian rhythms in plants (Bünning 1936). Since then, studies of plants (Nanda & Hamner 1958) and mammals (Hamner 1963; Elliott *et al.* 1972; Grocock & Clarke 1974; Stetson *et al.* 1976; Wada 1979) have established a role for circadian rhythms in day-length measurement. When house finches are exposed to a range of light cycles each containing a 6-h of light coupled to various length of darkness (6, 18, 30, 42, 54, and 66 hours of darkness) to give overall cycles ranging from about 12 to 72 hours, the 6-h light period coupled with dark periods in cycle lengths of 24, 48, and 72 hours does not stimulate testicular growth (a long-day photoperiodic response), but induce the response in cycles of 12, 36, and 60 hours (Hamner 1963). Thus, timing of a 6-h of light, which can trigger testicular growth (called as photoinducible phase), appearing at

24-h intervals was suggested to be important (Fig. G1). Similar observations were also reported gonadotropin secretion in the white-crowned sparrow (Follett *et al.* 1974) and testis function in Syrian hamsters (Elliott *et al.* 1972). In addition, the lesions of the SCN disrupt the testicular responses to day-length in Syrian hamsters (Rusak & Morin 1976; Stetson & Watson-Whitmyre 1976). All of these observations clearly suggest the involvement of the circadian clock in day-length measurement.

Melatonin represents light information in mammals

Mammals perceive light with the eyes and the light signals are transmitted to the pineal via a multisynaptic pathway including the retinohypothalamic tract, the SCN, and the sympathetic nervous system. Under the control of this pathway, including the exogenous light input and the circadian clock, the pineal organ synthesizes and secretes melatonin during the dark phase (Reiter 1980; Arendt 1998) (Fig. G2). Therefore, when the night length is long, the duration of melatonin secretion is long (winter) and when the night length is short, the duration of melatonin secretion is short (summer). Thus, melatonin is the endocrine representation of the period of darkness, inversely reflecting day-length. Furthermore, pinealectomy (disruption of melatonin secretion) abolishes seasonal responses in hamsters (Hoffman & Reiter 1965; Hoffmann 1979). Melatonin injections given at dusk or before dawn are sufficient to induce a short day-length (short-day) typical gonadal response in Syrian hamsters kept under long day-length (long-day) conditions (Turek *et al.* 1975; Tamarkin *et al.* 1976). These observations support that melatonin transmits external light information as darkness information and plays an important role in photoperiodism. Although eyes are believed to be the only photoreceptor organs in mammals, and removal of the eyes abolishes the photoperiodic response (Reiter 1980), removal of the eyes does not affect photoperiodic response in birds (Benoit 1935a, 1935b; Foster & Soni 1998). Instead, birds perceive light via deep brain photoreceptors expressed in the brain, and Opsin-5 and VA-opsin are identified as deep brain photoreceptors (Halford *et al.* 2009; Nakane *et al.* 2010; Yamashita *et al.* 2010). Recently it is reported that Opsin-5 is involved in *TSH*β induction (Nakane *et al.* 2014).

In summary, both internal time information and environmental light information are necessary for day-length measurement. However, the integration process of this information remains largely unknown.

The pars tuberalis is an important tissue for day-length measurement

In vitro autoradiography and *in situ* hybridization studies have identified areas of the brain that express melatonin receptors and could potentially receive seasonal variations in daily nocturnal melatonin profiles. The pars tuberalis (PT) is a common site expressing melatonin receptors among mammals (sheep, deers, goats, rabbits, rats, Syrian hamsters, Djungarian hamsters, mice, and ferrets), including seasonal animals

(Morgan *et al.* 1994) (Fig. G2). The PT is a tissue composed of highly vascularized multicellular tubes surrounding the pituitary stalk (Stoeckel & Porte 1984) (Fig. G3). The PT is an interface between the hypothalamus, which regulates reproduction, and the pars distalis (PD), which is part of the pituitary and contains the bulk of the hormone-secreting cells. Two melatonin receptor subtypes, MT1 and MT2, are identified in mammals. Both MT1 and MT2 belong to the large G protein-coupled, seven-transmembrane protein family (Dubocovich *et al.* 2003). MT1 appears to be the highly dominant subtype in the PT because targeted disruption of its gene in mice leads to undetectable levels of an 2-[^{125}I]iodomelatonin binding (Liu *et al.* 1997), while MT2 is believed to be naturally nonfunctional in highly photoperiodic species such as Siberian hamster (Weaver *et al.* 1996). Therefore, it is believed that the PT is responsible for day-length measurement thorough MT1.

The PT consists of several types of cells including PT-specific secretory cells, follicular cells, and PD-like endocrine cells (Stoeckel *et al.* 1979; Rudolf *et al.* 1993). PT-specific secretory cells are a major content of the PT and they show immunoreactivity of thyroid-stimulating hormone (TSH), thus called as thyrotrophs (Wittkowski *et al.* 1999). Generally, the PD is a major organ that secretes TSH, and TSH-secreting cells in the PD are also called as thyrotrophs. TSH is a heterodimer of *thyroid-stimulating hormone beta subunit* (*TSH*β), which is a unique beta subunit of TSH, and *common glycoprotein alpha subunit* (*Cga*), which is a common alpha subunit of TSH, follicle stimulating hormone and luteinizing hormone. However, regulatory mechanisms of TSH in the PT thyrotrophs are different from that in the PD thyrotrophs. TSH in the PD thyrotrophs is controlled by the negative feedback loop of the hypothalamus–pituitary–thyroid (HPT) axis, and they show responsiveness to thyroid releasing hormone (TRH) and thyroid hormone (TH). In contrast, the *TSH*β expression in ovine PT did not change by TRH and TH treatment, because of the lack of TRH and TH receptors or transcription factor *Pit-1*, which induces *TSH*β in the PD (Bockmann *et al.* 1997). These observations suggest that thyrotrophs in the PT are not controlled by the negative feedback loop of the HPT axis. On the other hand, TSH immunoreactivity in the PT of the Djungarian hamster changed by day-length (Wittkowski *et al.* 1988). Taken together, the tissue apparently responds to light conditions, possibly through melatonin signal, rather than the hormonal feedback loop.

It is also reported that circadian clock genes are expressed and oscillating in the PT (Ansari *et al.* 2009), and the expressions are apparently affected by melatonin signal (Fig. G3). It was shown that MT1 and *ROR*β, which is one of the circadian clock genes, are co-expressed in the rat PT (Klosen *et al.* 2002). Pinealectomy abolished expression of *period 1* (*Per1*) (Messager *et al.* 2001) in the PT, and rhythmic expressions of circadian clock genes such as *Per1*, *Cry1*, *Clock*, and *Bmal1* were also abolished in the PT of MT1 knockout mice (von Gall *et al.* 2002; Jilg *et al.* 2005). These reports indicate that the circadian

clock in the PT is affected by melatonin. However, the mechanism by which light information such as melatonin is decoded within the PT is still unknown.

2. General view of molecular mechanism for day-length detection

TSH represents long-day detection in the PT

It was known for long time that administration of TH mimics the physiological effects of long-day condition (Follett & Nicholls 1985; Goldsmith & Nicholls 1992) such as testicular growth of Japanese quail, (*Coturnix japonica*), which is the obvious seasonal change of the animal. The quail is a well-used model for studying photoperiodism, because the animal shows such rapid reproductive response to changing day-length, and functional gene expression analysis in the quail revealed the role of TSH and TH on the reproductive function (Yoshimura *et al.* 2003; Nakao *et al.* 2008). As summarized in Fig. G4, it was found that *TSH*β gene was rapidly induced in the PT within several hours after exposure of the animal to the long-day condition. In contrast, *Cga* was constantly expressed in the PT. Because TSH is believed to act on TSH receptor (TSHR) as a heterodimer peptide hormone, functional dynamics of TSH heterodimer are dependent on the expression levels of *TSH*β rather than *Cga*. The TSH heterodimer from the PT binds to TSHR expressed in the ependymal cell layer (EC) of the third ventricle and regulates the expression of *type 2 iodothyronine deiodinase* (*Dio2*) and *type 3 deiosinase* (*Dio3*). Dio2, a thyroid hormone activating enzyme, then converts the prohormone thyroxine (T4) to bioactive triiodothyroine (T3). Interestingly, blood concentration of TH did not alter between short-day and long-day conditions. Thus, induction of *Dio2* by TSH might cause local increase in T3 concentration under the long-day condition and photoperiodic responses. Furthermore, intracerebroventricular infusion of T3 or TSH mimics photoperiodically induced testicular growth (Yoshimura *et al.* 2003; Nakao *et al.* 2008). These findings suggested a new role of TSH and TH on reproduction in quail's photoperiodism and TSH is considered as a photoperiodic marker of long-day detection (Fig. G4).

TSH responsiveness in mammalian photoperiodism

This TSH-Dio2 molecular mechanism has also been conserved among mammals, including the mouse (Ono *et al.* 2008), Syrian hamster (Yasuo *et al.* 2010), European hamster (Hanon *et al.* 2010), sheep (Hanon *et al.* 2008) and rat (Ross *et al.* 2011). In general, laboratory mice are considered to be non-seasonal animals because they do not show photoperiodic phenotypes such as seasonal reproduction. Furthermore, many strains of mice have genetic mutations of two rate-limiting enzymes for melatonin synthesis from serotonin (arylalkylamine N-acetyltransferase (AANAT) and hydroxyindole-*O*-methyltransferase (HIOMT)) and thus these strains lack melatonin productivity

(Ebihara *et al.* 1986; Goto *et al.* 1989). However, limited melatonin-proficient mice strains such as CBA/N display similar photoperiodic gene responses of *TSH*β and *Dio2* by long-day stimulation as seen in the quail, while such responses were not observed in the melatonin-deficient C57BL/6 strain (Ono *et al.* 2008; Masumoto *et al.* 2010). These observations indicate that the photoperiodic gene response is also conserved in mice, suggesting possible usefulness of the animal for photoperiodism study.

Melatonin regulates TSHβ expression in the PT

MT1 and *TSH*β are co-expressed in the same cell of the rat PT (Wittkowski *et al.* 1988; Klosen *et al.* 2002). Melatonin injection suppressed *TSH*β in the PT in mice, sheep and hamsters (Hanon *et al.* 2008; Ono *et al.* 2008; Yasuo *et al.* 2010). Furthermore, photoperiodic regulation of *Dio2* and *Dio3* expression is abolished in MT1 knockout mice (Yasuo *et al.* 2009). These reports suggest that melatonin-MT1 pathway potentially regulates *TSH*β and further downstream targets that are important for day-length measurement.

3. Upstream cascade of TSHβ

TSHβ induction mechanism

In the comprehensive gene expression analysis in Japanese quail, transcription cofactor *eyes absent 3* (*Eya3*) was also identified which shows rapid induction by long-day stimulation as seen in *TSH*β (Nakao *et al.* 2008). In melatonin-proficient mice, we reported that *Eya3* induction preceded *TSH*β induction, and *Eya3* transactivated *TSH*β with DNA binding transcription factor *sine oculis-related homeobox 1* (*Six1*) (Masumoto *et al.* 2010). Similar *Eya3*-*TSH*β mechanism was also found in sheep (Dardente *et al.* 2010).

Endogenous time determined by the circadian clock is as important as light signals for *TSH*β induction. We revealed the importance of timing of long-day stimulation for rapid *TSH*β induction. When mice were stimulated to long-day condition from short-day by advancing lights-on (late-night) or delaying lights-off (early-night) for 8 hours, late-night light stimulation immediately induced *TSH*β expression in the PT within several hours while early-night light stimulation did not increased *TSH*β within a day. Early-night light stimulation increased *TSH*β gradually over the 5 days (Fig. G5). It was indicated that late-night light stimulation is necessary for immediate *TSH*β induction in mammalian photoperiodism. Late-night time may be photoinducible phase in mammals.

We also found that expression patterns of circadian clock genes were not affected by late-light light stimulation while those expression patterns were perturbed by early-night light stimulation and the PT circadian time was gradually shifted over 5 days, as seen in jet-lag. It is implied that the PT circadian clock was entrained to the lights-off timing. Melatonin may be included this entrainment because the start

of melatonin secretion reflects lights-off timing and melatonin affects expression patterns of the circadian clock genes. Thus, expression patterns of clock genes may correspond to induction patterns of *TSH*β after long-day stimulation.

Furthermore, it was found that several circadian clock-controlled genes such as *thyrotroph embryonic factor* (*Tef*) and/or *hepatic leukemia factor* (*Hlf*) regulated *TSH*β expression synergistically with *Eya3* and *Six1* by *in vitro TSH*β promoter assay (Dardente *et al.* 2010; Masumoto *et al.* 2010) (Fig. G6). *Bmal1* and *Clock* also upregulated *TSH*β promoter activity (Unfried *et al.* 2010). These reports indicate that circadian clock genes control *TSH*β expression. Thus, endogenous time determined by circadian clock genes is important for optimal *TSH*β expression in photoperiodic reaction.

Intracellular melatonin signal transduction pathways in the PT

Molecules working in the downstream of MT1, a receptor subtype that is believed to mainly mediate photoperiodic responses conveyed by melatonin in the PT, are well studied by using ovine PT dissociation culture system. MT1 antagonize the induction of cAMP levels by adenylate cyclase (AC) activator forskolin (Morgan *et al.* 1989a; Morgan *et al.* 1989b). The effects were canceled by the G-protein inhibitor, pertussis-toxin (PTX), suggesting that MT1 couples to a G_i protein (Morgan *et al.* 1990). The G_i pathway of MT1 is believed to negatively regulate intracellular cAMP levels. Intriguingly, chronic melatonin treatment of PT cells sensitizes AC such that the induction of cAMP by forskolin can be greatly enhanced upon removal of melatonin (Barrett *et al.* 2000; Barrett *et al.* 2003). These results may suggest that sensitization of AC by the chronic melatonin treatment have some role for fine-tuning of day-length measurement. However, it is unknown whether the sensitizing effect is observed *in vivo*. The role of the sensitization and involving molecular mechanisms in the context of melatonin's action are not entirely clear.

Whereas melatonin signaling through MT1 leads to decrease in the intracellular cAMP levels, signals that increase cAMP levels are unknown. Although removal of melatonin increased intercellular cAMP concentration slightly in ovine PT cell culture (Hazlerigg *et al.* 1993), it may be insufficient to initiate an action *in vivo*. These observations may imply that melatonin acts indirectly to inhibit the effects of an unknown stimulatory factor, which increases cAMP levels in the PT.

How can connect the light, melatonin, and TSHβ?

Detailed pathway from light detection on the eyes to *TSH*β induction in the PT is unclear, whereas it is obvious that light regulates melatonin-MT1-*TSH*β pathway. Cyclic AMP signal transduction might be one of important mechanisms of inducting *TSH*β in the PT. However, there is no report showing light

dependency of the cAMP signal in the PT and the relationship between the cAMP signal and *TSH*β (Fig. G7).

Eya3 is also regulated by melatonin, because melatonin injection suppressed *Eya3* in the ovine PT (Dardente *et al.* 2010). Suppression of *Eya3* and *TSH*β expression in the PT by melatonin injection implies that an unknown stimulatory factor may reversely induce *Eya3* and *TSH*β thorough elevation of cAMP levels (Ono *et al.* 2008; Dardente *et al.* 2010; Masumoto *et al.* 2010; Yasuo *et al.* 2010). Light information for detecting long-day stimulation on the eyes might be transferred immediately to the PT and increase cAMP levels, because long-day stimulation induced *Eya3* in the PT within 4 hours (Masumoto *et al.* 2010). Circadian clock genes may also associate cAMP accumulation in the PT and/or *Eya3* and *TSH*β induction. However, signal transduction, which increases cAMP levels in the PT, remains unclear.

It is also unknown whether other signal transduction pathways such as calcium signals are involved in the PT. Thus, wide range of examinations of several molecular mechanisms is important. So far, it has been difficult to study these detailed molecular mechanisms because genetics were not available in model animals in photoperiodism study (Japanese quail, sheep, and so on). Recent studies revealing that melatonin-proficient mice possess photoperiodic gene response opened the door to apply techniques in mammalian genetics such as gene targeting and transgenic strategy to the research field. Thus, using mice was expected to promote studies about the molecular mechanisms in the PT and light information transferring pathway from the eyes to the PT.

4. Aim of this study: Identification of light information transferring molecules

Induction of *TSH*β in the PT is a marker for long-day detection as a result of integration of time information and light information. Light information-transferring molecule is unknown, whereas melatonin transfers darkness information to the PT. Furthermore, the detailed molecular mechanisms of induction of *Eya3* and *TSH*β in the PT are not clear as well. In this thesis, I focused on how *TSH*β expression in the PT is regulated by long-day stimulation because *TSH*β shows significant induction by long-day stimulation within several hours. Moreover, the photoperiodic role of *TSH*β is revealed, and the PT is an interface of seasonal reproduction. Conventional methods require an immense amount of care and time. For example, intraventricular administration of drugs or proteins, gene transfection or RNAi knockdown *in vivo* are needed for perturbing putative upstream molecule, and *in situ* hybridization or immunostaining are required for evaluating the effects of perturbation. These methods are not convenient for screening putative *TSH*β upstream molecules because upstream cascade of *TSH*β is largely unknown. Thus, I established screening systems of candidate upstream molecules of *TSH*β under conditions similar

to *in vivo* conditions. I performed preliminary screening of candidate upstream molecules of *TSH*β such as drugs targeting the cAMP signal, hormones, and so on by using this screening system, and I found that glutamic acid show *TSH*β-inducible activity. These results were consistent with previous study that show glutamic acid can induce *TSH*β in rat PT, suggesting that this screening system is functional (Aizawa *et al.* 2012). Unexpectedly, activators of cAMP-related molecules did not increase bioluminescence activities immediately after the treatment as seen in *TSH*β induction *in vivo* (Masumoto *et al.* 2010). From these results, I propose my screening system "*TSH*β real-time monitoring system" is a powerful tool to reveal photoperiodic molecular mechanisms.

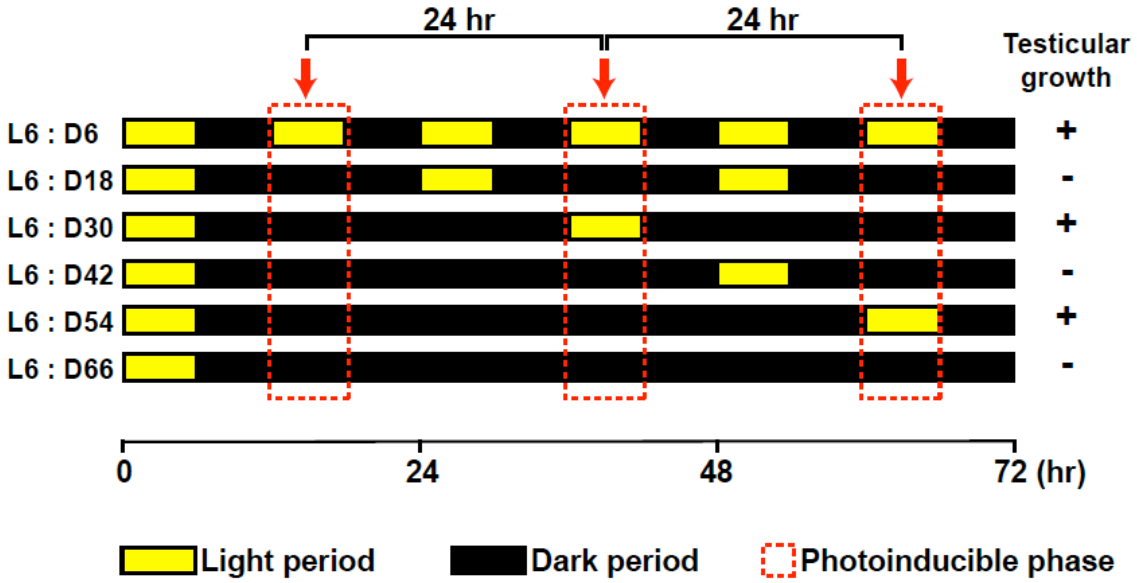

Figure G1. The circadian clock is involved in day-length measurement. Birds are exposed to a range of light cycles each containing a 6-h of light (L) coupled to various length of darkness [6, 18, 30, 42, 54, and 66 hours of darkness (D)]. Timing of a 6-h of light, which can trigger testicular growth, appeared at 24-h intervals (Hamner 1963). Light pulses given at a specific time of day called the "photoinducible phase" induce testicular growth in birds.

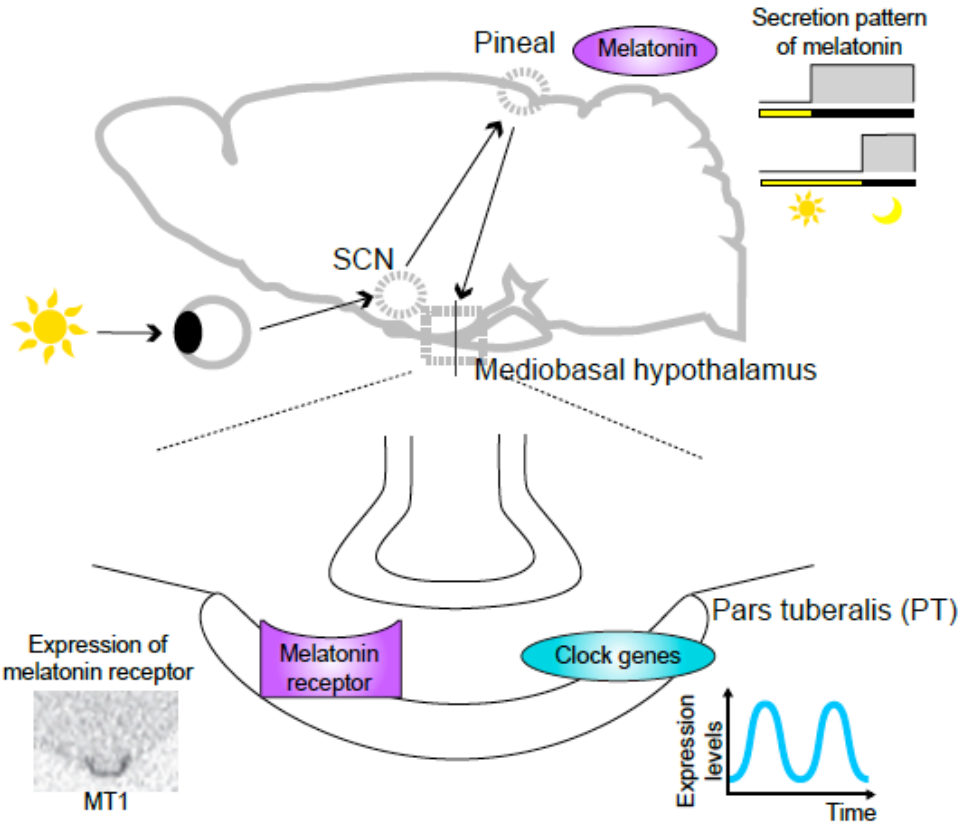

Figure G2. The day-length input pathway in mammals. Light is perceived by photoreceptors (melanopsin-containing ganglion cells) in the retina, which project directly to the suprachiasmatic nucleus (SCN). The SCN generates circadian rhythms and the SCN controls pineal melatonin production. Pineal melatonin is released in the bloodstream at night and reflects the night length of day-length. Melatonin binds to the melatonin receptors in the highly vascularized pars tuberalis (PT), where it also expresses circadian clock genes.

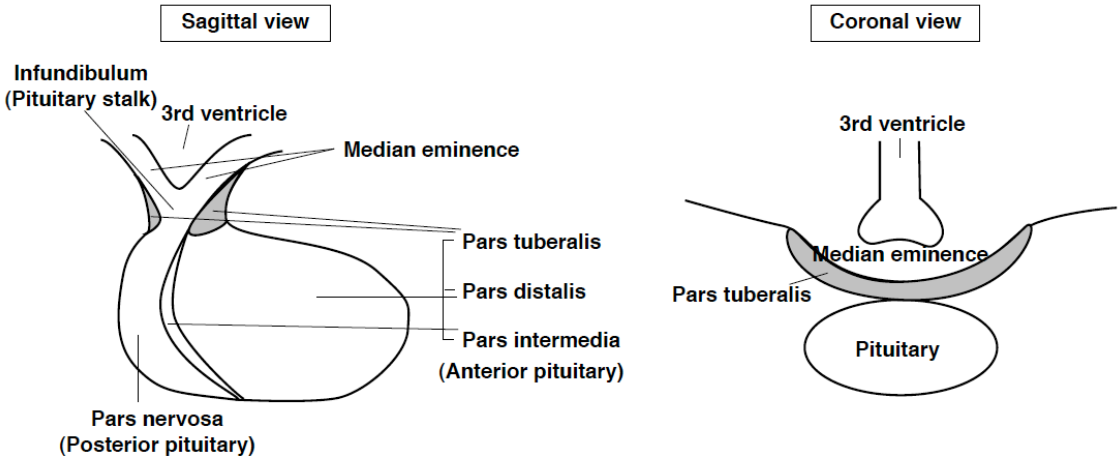

Figure G3. Schematic drawing of a sagittal section (left) and a coronal section (right) of the hypothalamus and the pituitary with special reference to topographic relations of the pars tuberalis (gray) of the anterior pituitary.

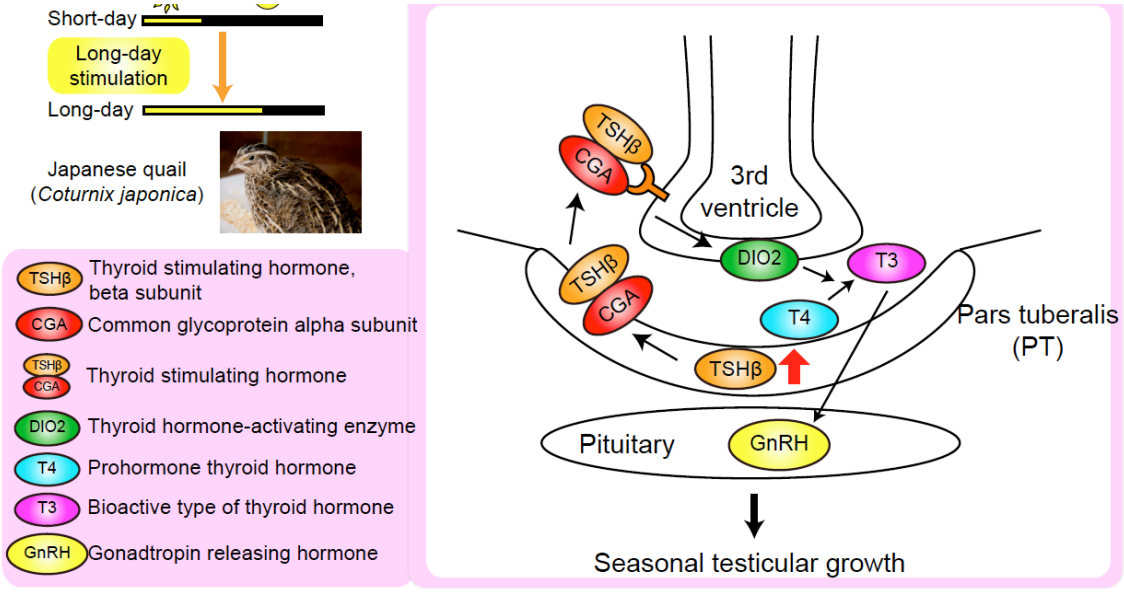

Figure G4. Photoperiodic signal transduction cascade in birds. Light information detected by deep brain photoreceptor is transmitted to the pars tuberalis (PT), inducing thyroid-stimulating hormone (TSH). TSH in the PT acts on the ependymal cells to induce thyroid hormone-activating enzyme, *type 2 deiodinase* (*Dio2*). Triiodothyronine (T3) converted from thyroxine (T4) by Dio2 regulates gonadotropin releasing hormone (GnRH) secretion and hence gonadotropin secretion from the anterior pituitary gland.

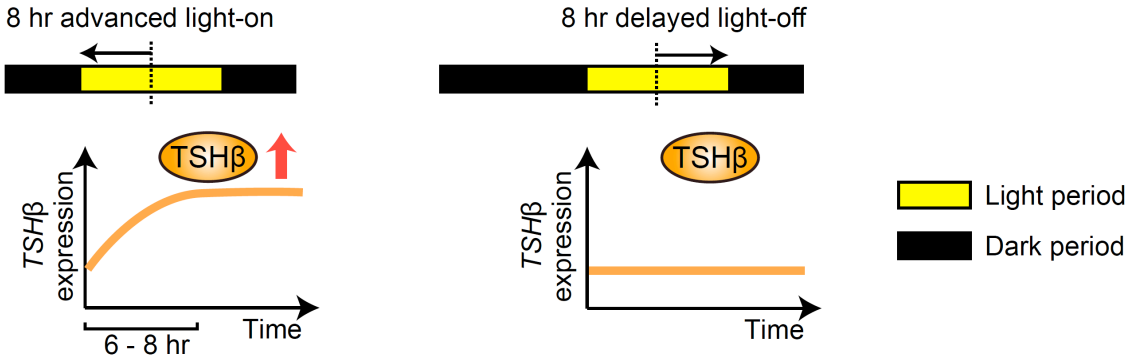

Figure G5. Light stimulation at a specific time can induce *TSH*β rapidly. 8-h advanced lights-on (late-night light) induced *TSH*β within several hours. The PT circadian clock was not affected by late-light stimulation. In contrast, 8-h delayed lights-off (early-night light) did not induce *TSH*β within the first day. The PT circadian clock was perturbed by early-light stimulation and it was entrained gradually. Modified from Masumoto, K. H. *et al*. (2010) *Curr Biol*.

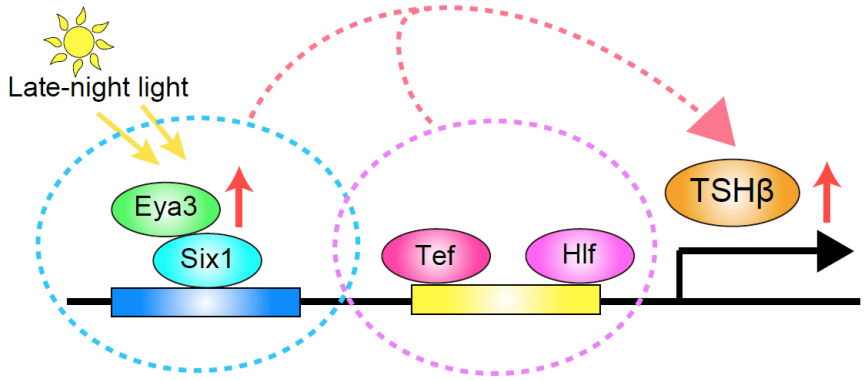

Figure G6. Acute induction of *Eya3* by late-night light stimulation triggers *TSH*β expression in photoperiodism. *Eya3* and its partner *Six1* synergistically activate *TSH*β expression and that this activation is further enhanced by *Tef* and/or *Hlf*.

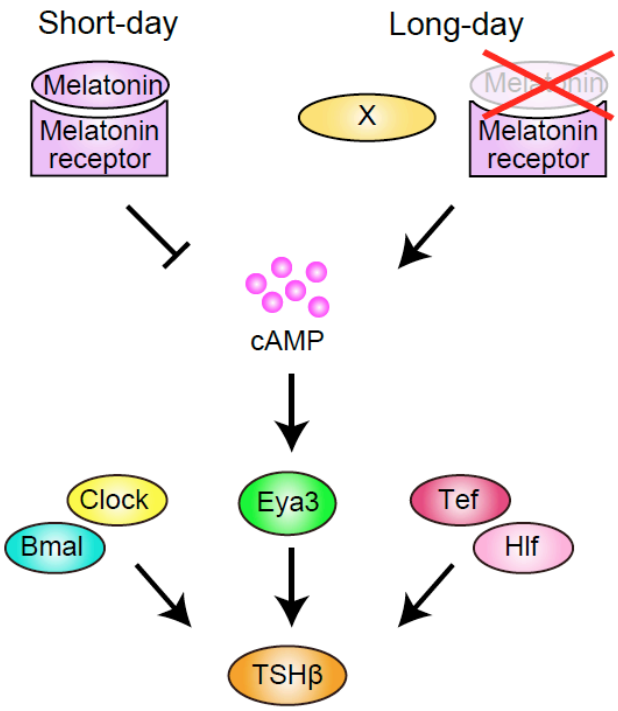

Figure G7. A model for interactions between melatonin, cAMP, *TSH*β, and other transcription factors in the PT cells. In short-day condition, melatonin suppresses intercellular cAMP concentration thorough MT1. This may decrease *Eya3* and *TSH*β expression. In contrast, sutimulator X, may elevates intercellular cAMP concentration and may induce *Eya3* and *TSH*β under long-day condition. *Eya3* transactivated *TSH*β with DNA binding transcription factor *Six1*. Several circadian clock-controlled genes such as *Tef* and/or *Hlf* regulated *TSH*β expression synergistically with *Eya3* and *Six1*. Circadian clock genes *Bmal1* and *Clock* also upregulated *TSH*β promoter activity.

References

Aizawa, S., Sakai, T. & Sakata, I. (2012) Glutamine and glutamic acid enhance thyroid-stimulating hormone beta subunit mRNA expression in the rat pars tuberalis. *J Endocrinol* **212**, 383-394.

Albrecht, U. (2002) Invited review: regulation of mammalian circadian clock genes. *J Appl Physiol* **92**, 1348-1355.

Ansari, N., Agathagelidis, M., Lee, C., Korf, H.W. & von Gall, C. (2009) Differential maturation of circadian rhythms in clock gene proteins in the suprachiasmatic nucleus and the pars tuberalis during mouse ontogeny. *Eur J Neurosci* **29**, 477-489.

Arendt, J. (1998) Melatonin and the pineal gland: influence on mammalian seasonal and circadian physiology. *Rev Reprod* **3**, 13-22.

Bünning, E. (1936) Die endogene Tagesrhythmik als Grundlage der photoperiodischen Reaktion. *Ber. Dtsch. Bot. Ges.* **54**, 590–607.

Barrett, P., Choi, W.S., Morris, M. & Morgan, P. (2000) A role for tyrosine phosphorylation in the regulation and sensitization of adenylate cyclase by melatonin. *FASEB J* **14**, 1619-1628.

Barrett, P., Schuster, C., Mercer, J. & Morgan, P.J. (2003) Sensitization: a mechanism for melatonin action in the pars tuberalis. *J Neuroendocrinol* **15**, 415-421.

Benoit, J. (1935a) Le role des yeux dans l'action stimulante de la lumiere sur le developpement testiculaire chez le canard. *Comptes Rendus des Seances de la Societe de Physique et de ses Filiales* **118**, 669–671.

Benoit, J. (1935b) Stimulation par la lumiere artificielle du developpement testiculaire chez des canards aveugles par section du nerf optique. *Comptes Rendus des Seances de la Societe de Physique et de ses Filiales* **120**, 133 - 136.

Bockmann, J., Bockers, T.M., Winter, C., Wittkowski, W., Winterhoff, H., Deufel, T. & Kreutz, M.R. (1997) Thyrotropin expression in hypophyseal pars tuberalis-specific cells is 3,5,3'-triiodothyronine, thyrotropin-releasing hormone, and pit-1 independent. *Endocrinology* **138**, 1019-1028.

Dardente, H., Wyse, C.A., Birnie, M.J., Dupre, S.M., Loudon, A.S., Lincoln, G.A. & Hazlerigg, D.G. (2010) A molecular switch for photoperiod responsiveness in mammals. *Curr Biol* **20**, 2193-2198.

Dubocovich, M.L., Rivera-Bermudez, M.A., Gerdin, M.J. & Masana, M.I. (2003) Molecular pharmacology, regulation and function of mammalian melatonin receptors. *Front Biosci* **8**, d1093-1108.

Ebihara, S., Marks, T., Hudson, D.J. & Menaker, M. (1986) Genetic control of melatonin synthesis in the pineal gland of the mouse. *Science* **231**, 491-493.

Elliott, J.A., Stetson, M.H. & Menaker, M. (1972) Regulation of testis function in golden hamsters: a circadian clock measures photoperiodic time. *Science* **178**, 771-773.

Follett, B.K., Mattocks, P.W., Jr. & Farner, D.S. (1974) Circadian function in the photoperiodic induction of gonadotropin secretion in the white-crowned sparrow, Zonotrichia leucophrys gambelii. *Proc Natl Acad Sci U S A* **71**, 1666-1669.

Follett, B.K. & Nicholls, T.J. (1985) Influences of thyroidectomy and thyroxine replacement on photoperiodically controlled reproduction in quail. *J Endocrinol* **107**, 211-221.

Foster, R.G. & Soni, B.G. (1998) Extraretinal photoreceptors and their regulation of temporal physiology. *Rev Reprod* **3**, 145-150.

Goldsmith, A.R. & Nicholls, T.J. (1992) Thyroxine Effects upon Reproduction, Prolactin Secretion and Plumage Moult in Intact and in Thyroidectomised European Starlings Sturnus vulgaris. *Ornis Scandinavica* **23**, 398–404.

Goto, M., Oshima, I., Tomita, T. & Ebihara, S. (1989) Melatonin content of the pineal gland in different mouse strains. *J Pineal Res* **7**, 195-204.

Grocock, C.A. & Clarke, J.R. (1974) Photoperiodic control of testis activity in the vole, Microtus agrestis. *J Reprod Fertil* **39**, 337-347.

Halford, S., Pires, S.S., Turton, M., Zheng, L., Gonzalez-Menendez, I., Davies, W.L., Peirson, S.N., Garcia-Fernandez, J.M., Hankins, M.W. & Foster, R.G. (2009) VA opsin-based photoreceptors in the hypothalamus of birds. *Curr Biol* **19**, 1396-1402.

Hamner, W.M. (1963) Diurnal Rhythm and Photoperiodism in Testicular Recrudescence of the House Finch. *Science* **142**, 1294-1295.

Hanon, E.A., Lincoln, G.A., Fustin, J.M., Dardente, H., Masson-Pevet, M., Morgan, P.J. & Hazlerigg, D.G. (2008) Ancestral TSH mechanism signals summer in a photoperiodic mammal. *Curr Biol* **18**, 1147-1152.

Hanon, E.A., Routledge, K., Dardente, H., Masson-Pevet, M., Morgan, P.J. & Hazlerigg, D.G. (2010) Effect of photoperiod on the thyroid-stimulating hormone neuroendocrine system in the European hamster (Cricetus cricetus). *J Neuroendocrinol* **22**, 51-55.

Hazlerigg, D.G., Gonzalez-Brito, A., Lawson, W., Hastings, M.H. & Morgan, P.J. (1993) Prolonged exposure to melatonin leads to time-dependent sensitization of adenylate cyclase and down-regulates melatonin receptors in pars tuberalis cells from ovine pituitary. *Endocrinology* **132**, 285-292.

Hoffman, R.A. & Reiter, R.J. (1965) Pineal Gland: Influence on Gonads of Male Hamsters. *Science* **148**, 1609-1611.

Hoffmann, K. (1979) Photoperiod, pineal, melatonin and reproduction in hamsters. *Prog Brain Res* **52**,

397-415.

Jilg, A., Moek, J., Weaver, D.R., Korf, H.W., Stehle, J.H. & von Gall, C. (2005) Rhythms in clock proteins in the mouse pars tuberalis depend on MT1 melatonin receptor signalling. *Eur J Neurosci* **22**, 2845-2854.

Klosen, P., Bienvenu, C., Demarteau, O., Dardente, H., Guerrero, H., Pevet, P. & Masson-Pevet, M. (2002) The mt1 melatonin receptor and RORbeta receptor are co-localized in specific TSH-immunoreactive cells in the pars tuberalis of the rat pituitary. *J Histochem Cytochem* **50**, 1647-1657.

Liu, C., Weaver, D.R., Jin, X., Shearman, L.P., Pieschl, R.L., Gribkoff, V.K. & Reppert, S.M. (1997) Molecular dissection of two distinct actions of melatonin on the suprachiasmatic circadian clock. *Neuron* **19**, 91-102.

Masumoto, K.H., Ukai-Tadenuma, M., Kasukawa, T., Nagano, M., Uno, K.D., Tsujino, K., Horikawa, K., Shigeyoshi, Y. & Ueda, H.R. (2010) Acute induction of Eya3 by late-night light stimulation triggers TSHbeta expression in photoperiodism. *Curr Biol* **20**, 2199-2206.

Messager, S., Garabette, M.L., Hastings, M.H. & Hazlerigg, D.G. (2001) Tissue-specific abolition of Per1 expression in the pars tuberalis by pinealectomy in the Syrian hamster. *Neuroreport* **12**, 579-582.

Morgan, P.J., Barrett, P., Howell, H.E. & Helliwell, R. (1994) Melatonin receptors: localization, molecular pharmacology and physiological significance. *Neurochem Int* **24**, 101-146.

Morgan, P.J., Davidson, G., Lawson, W. & Barrett, P. (1990) Both pertussis toxin-sensitive and insensitive g-proteins link melatonin receptor to inhibition of adenylate cyclase in the ovine pars tuberalis. *J Neuroendocrinol* **2**, 773-776.

Morgan, P.J., Lawson, W., Davidson, G. & Howell, H.E. (1989a) MELATONIN INHIBITS CYCLIC AMP PRODUCTION IN CULTURED OVINE PARS TUBERALIS CELLS. *Journal of Molecular Endocrinology* **3**, R5-R8.

Morgan, P.J., Williams, L.M., Davidson, G., Lawson, W. & Howell, E. (1989b) Melatonin receptors on ovine pars tuberalis: characterization and autoradiographicai localization. *J Neuroendocrinol* **1**, 1-4.

Nakane, Y., Ikegami, K., Ono, H., Yamamoto, N., Yoshida, S., Hirunagi, K., Ebihara, S., Kubo, Y. & Yoshimura, T. (2010) A mammalian neural tissue opsin (Opsin 5) is a deep brain photoreceptor in birds. *Proc Natl Acad Sci U S A* **107**, 15264-15268.

Nakane, Y., Shimmura, T., Abe, H. & Yoshimura, T. (2014) Intrinsic photosensitivity of a deep brain photoreceptor. *Curr Biol* **24**, R596-597.

Nakao, N., Ono, H., Yamamura, T. *et al.* (2008) Thyrotrophin in the pars tuberalis triggers photoperiodic response. *Nature* **452**, 317-322.

Nanda, K.K. & Hamner, K.C. (1958) Studies on the Nature of the Endogenous Rhythm Affecting

Photoperiodic Response of Biloxi Soybean. *Botanical Gazette* **120**, 14 - 25.

Ono, H., Hoshino, Y., Yasuo, S., Watanabe, M., Nakane, Y., Murai, A., Ebihara, S., Korf, H.W. & Yoshimura, T. (2008) Involvement of thyrotropin in photoperiodic signal transduction in mice. *Proc Natl Acad Sci U S A* **105**, 18238-18242.

Reiter, R.J. (1980) The pineal and its hormones in the control of reproduction in mammals. *Endocr Rev* **1**, 109-131.

Ross, A.W., Helfer, G., Russell, L., Darras, V.M. & Morgan, P.J. (2011) Thyroid hormone signalling genes are regulated by photoperiod in the hypothalamus of F344 rats. *PLoS One* **6**, e21351.

Rudolf, T., Filler, T. & Wittkowski, W. (1993) Pars tuberalis specific cells within the pars distalis of the adenohypophysis. An ontogenetic study. *Ann Anat* **175**, 171-176.

Rusak, B. & Morin, L.P. (1976) Testicular responses to photoperiod are blocked by lesions of the suprachiasmatic nuclei in golden hamsters. *Biol Reprod* **15**, 366-374.

Stetson, M.H., Matt, K.S. & Watson-Whitmyre, M. (1976) Photoperiodism and reproduction in golden hamsters: circadian organization and the termination of photorefractoriness. *Biol Reprod* **14**, 531-537.

Stetson, M.H. & Watson-Whitmyre, M. (1976) Nucleus suprachiasmaticus: the biological clock in the hamster? *Science* **191**, 197-199.

Stoeckel, M.E., Hindelang-Gertner, C. & Porte, A. (1979) Embryonic development and secretory differentiation in the pars tuberalis of the mouse hypophysis. *Cell Tissue Res* **198**, 465-476.

Stoeckel, M.E. & Porte, A. (1984) Fine structure and development of the pars tuberalis in mammals. *Ultrastructure of Endocrine Cells and Ttissues* **1**, 29 - 38

Tamarkin, L., Westrom, W.K., Hamill, A.I. & Goldman, B.D. (1976) Effect of melatonin on the reproductive systems of male and female Syrian hamsters: a diurnal rhythm in sensitivity to melatonin. *Endocrinology* **99**, 1534-1541.

Turek, F.W., Desjardins, C. & Menaker, M. (1975) Melatonin: antigonadal and progonadal effects in male golden hamsters. *Science* **190**, 280-282.

Ueda, H.R., Hayashi, S., Chen, W., Sano, M., Machida, M., Shigeyoshi, Y., Iino, M. & Hashimoto, S. (2005) System-level identification of transcriptional circuits underlying mammalian circadian clocks. *Nat Genet* **37**, 187-192.

Unfried, C., Burbach, G., Korf, H.W. & von Gall, C. (2010) Melatonin receptor 1-dependent gene expression in the mouse pars tuberalis as revealed by cDNA microarray analysis and in situ hybridization. *J Pineal Res* **48**, 148-156.

von Gall, C., Garabette, M.L., Kell, C.A., Frenzel, S., Dehghani, F., Schumm-Draeger, P.M., Weaver, D.R., Korf, H.W., Hastings, M.H. & Stehle, J.H. (2002) Rhythmic gene expression in pituitary depends

on heterologous sensitization by the neurohormone melatonin. *Nat Neurosci* **5**, 234-238.

Wada, M. (1979) Photoperiodic control of LH secretion in Japanese quail with special reference to the photoinducible phase. *Gen Comp Endocrinol* **39**, 141-149.

Weaver, D.R., Liu, C. & Reppert, S.M. (1996) Nature's knockout: the Mel1b receptor is not necessary for reproductive and circadian responses to melatonin in Siberian hamsters. *Mol Endocrinol* **10**, 1478-1487.

Welsh, D.K., Takahashi, J.S. & Kay, S.A. (2010) Suprachiasmatic nucleus: cell autonomy and network properties. *Annu Rev Physiol* **72**, 551-577.

Wittkowski, W., Bergmann, M., Hoffmann, K. & Pera, F. (1988) Photoperiod-dependent changes in TSH-like immunoreactivity of cells in the hypophysial pars tuberalis of the Djungarian hamster, Phodopus sungorus. *Cell Tissue Res* **251**, 183-187.

Wittkowski, W., Bockmann, J., Kreutz, M.R. & Bockers, T.M. (1999) Cell and molecular biology of the pars tuberalis of the pituitary. *Int Rev Cytol* **185**, 157-194.

Yamashita, T., Ohuchi, H., Tomonari, S., Ikeda, K., Sakai, K. & Shichida, Y. (2010) Opn5 is a UV-sensitive bistable pigment that couples with Gi subtype of G protein. *Proc Natl Acad Sci U S A* **107**, 22084-22089.

Yasuo, S., Yoshimura, T., Ebihara, S. & Korf, H.W. (2009) Melatonin transmits photoperiodic signals through the MT1 melatonin receptor. *J Neurosci* **29**, 2885-2889.

Yasuo, S., Yoshimura, T., Ebihara, S. & Korf, H.W. (2010) Photoperiodic control of TSH-beta expression in the mammalian pars tuberalis has different impacts on the induction and suppression of the hypothalamo-hypopysial gonadal axis. *J Neuroendocrinol* **22**, 43-50.

Yoshimura, T., Yasuo, S., Watanabe, M., Iigo, M., Yamamura, T., Hirunagi, K. & Ebihara, S. (2003) Light-induced hormone conversion of T4 to T3 regulates photoperiodic response of gonads in birds. *Nature* **426**, 178-181.

Establishment of TSHβ real-time monitoring system in mammalian photoperiodism

Introduction

Many organisms adapt their physiological functions and behaviors to seasonal environmental changes by measuring day length, a biological process known as photoperiodism (Dawson *et al.* 2001; Ebling & Barrett 2008; Revel *et al.* 2009). Integration of external light information and endogenous time mediated by circadian clock genes (clockwork genes) is important for the photoperiodic responses (Hamner 1963; Pittendrigh & Minis 1964).

The pars tuberalis (PT) of the pituitary gland may be responsible for the photoperiodic responses because of the high expression levels of the clockwork genes and melatonin receptor 1a (MT1) in the PT (Morgan & Williams 1996; Lincoln *et al.* 2003; Ikegami & Yoshimura 2012). In mammals, it is suggested that nocturnal melatonin conveys darkness information to the PT, but the molecules conveying light information remain unknown (Hoffman & Reiter 1965; Morgan & Williams 1996). In a recent study, *thyroid-stimulating hormone beta subunit* (*TSH*β) gene was found to be rapidly induced by long-day stimulation in the PT and the product of *TSH*β, thyroid-stimulating hormone (TSH), has a functional role in seasonal testicular growth in birds (Yoshimura *et al.* 2003; Nakao *et al.* 2008). This *TSH*β induction is conserved even in mammals including melatonin-proficient mice (Hanon *et al.* 2008; Ono *et al.* 2008; Dardente *et al.* 2010; Dupre *et al.* 2010; Masumoto *et al.* 2010; Yasuo *et al.* 2010). Therefore, *TSH*β is a key factor for day-length detection and controls seasonal physiological changes.

Delivery of light information from the retina to the PT is an important pathway for inducing *TSH*β expression and regulating photoperiodic responses. Indeed, removal of the eyes, the suprachiasmatic nucleus or the pineal gland disrupts testicular responses in hamsters (Hoffman & Reiter 1965; Rusak & Morin 1976; Stetson & Watson-Whitmyre 1976). In the mouse PT, long-day stimulation induces a transcription cofactor *eyes absent 3* (*Eya3*) (Masumoto *et al.* 2010). This molecule regulates *TSH*β expression with DNA-binding transcription factor *sine oculis-related homeobox 1* (*Six1*) and several clockwork genes such as *thyrotroph embryonic factor* (*Tef*) and/or *hepatic leukemia factor* (*Hlf*) (Dardente *et al.* 2010; Masumoto *et al.* 2010). These molecular mechanisms have also been found in sheep (Dardente *et al.* 2010; Dupre *et al.* 2010). On the other hand, darkness information is mediated by melatonin that suppresses *Eya3* and *TSH*β expression in sheep and mice, respectively (Ono *et al.* 2008; Unfried *et al.* 2009; Dardente *et al.* 2010; Yasuo *et al.* 2010). Thus, the regulation of *Eya3* by external light conditions is critical to control *TSH*β expression for photoperiodism. However, the intracellular and

extracellular signals that transfer the external light information to the PT to regulate *Eya3* and *TSH*β expression remain unknown.

In this study, I focused on how *TSH*β expression in the PT is regulated by long-day stimuli. To accomplish this, I established a real-time monitoring system for measuring *TSH*β expression dynamics for the purpose of screening candidate light information-transferring signals in the PT. I generated a genetic mouse model in which *TSH*β expression dynamics in the PT can be visualized by bioluminescence. Treatment of cultured PT slices with melatonin decreased bioluminescence activities, and these results showed that PT slices can response to melatonin in my culture condition. Furthermore, I performed preliminary screening for candidate upstream molecules of *TSH*β such as drugs targeting the cAMP signal by using this *TSH*β real-time monitoring system, and I found that glutamic acid increased bioluminescence activities acutely, consistent with previous study (Aizawa *et al.* 2012). In contrast, activators of cAMP-related molecules did not increase bioluminescence activities immediately after the treatment as seen in *TSH*β induction *in vivo*. These observations suggest that this screening system could response to external signals. Thus, my mouse model could be used to search for molecules that relay external light signals in the PT.

Results

1. Establishment of TSHβ real-time monitoring system in mammalian photoperiodism

Generation of TSHβ^{Luc} mice

To monitor *TSH*β expression in the PT, I applied a knock-in approach in which 5′ exon of *TSH*β-coding sequence was knocked out and replaced with a firefly *Luciferase* (*Luc*) gene (Fig. 1A). In this scheme, the luc activity represents direct transcription from the endogenous *TSH*β promoter. Southern blot analysis confirmed that the desired mutation was successfully introduced (Fig. 1B, left), and genotypes of offspring were routinely analyzed by PCR (Fig. 1B, right). Animals were backcrossed and maintained on a CBA/N background because unlike the more common C57BL/6 strain, CBA/N mice maintain melatonin proficiency (Ebihara *et al.* 1986; Nakahara *et al.* 2003).

To verify the loss of *TSH*β transcript, I performed quantitative RT-PCR (qPCR) to measure the expression levels of *TSH*β and its related genes in the pituitary composed of the anterior and posterior lobes, where the highest *TSH*β expression level in the brain was observed (Kasukawa *et al.* 2011). By using primers aligned within exon 4, which was deleted by the targeting (Fig. 1A), *TSH*β mRNA was undetectable in homozygous *TSH*β^{Luc} mice. On the other hand, only 12% decrease in *TSH*β expression levels was observed in heterozygous *TSH*β^{Luc} mice compared with wild-type mice (Fig. 1C). The expression levels of *common glycoprotein* α*-subunit* (*Cga*), the alpha subunit of TSH, were not different between wild-type and heterozygous *TSH*β^{Luc} mice, but there was a 4-fold increase in homozygous *TSH*β^{Luc} mice (Fig. 1C), suggesting antirepression of negative feedback loop due to the disruption of the TSH heterodimer. *Luc* expression levels were observed in heterozygous *TSH*β^{Luc} mice, significantly increased in homozygous *TSH*β^{Luc} mice and undetectable in wild-type mice, also suggesting the disruption of the TSH heterodimer (Fig. 1C). One hundred and thirty-seven offspring from heterozygous matings were examined. 30 animals were wild-type (21%), 85 heterozygous (53%) and 35 animals homozygous *TSH*β^{Luc} mice (26%). These results are consistent with single-gene Mendelian inheritance, indicating that the *TSH*β null mutation did not lead to fetal loss and *TSH*β was not necessary for embryonic growth or viability. However, male and female homozygous *TSH*β^{Luc} mice were sterile. Weekly body weight results showed that homozygous *TSH*β^{Luc} mice display a low rate of growth, whereas heterozygous *TSH*β^{Luc} mice were indistinguishable from wild-type mice (Fig. 1D). These results indicate that slightly reduced *TSH*β expression and *Luc* expression do not affect the physiology in heterozygous *TSH*β^{Luc} mice. In addition, growth retardation in homozygous *TSH*β^{Luc} mice was recovered by supplementation with 100 ppm thyroid powder, consistent with the observation in TSH receptor (TSHR) knockout mice (Marians *et al.* 2002) (Fig. 1D). From these observations, I concluded that

phenotypes of heterozygous *TSH*β^{Luc} mice are comparable with those of wild-type mice.

Relationship between TSHβ and Luc expression in TSHβ^{Luc} mice

Next, I checked whether the knock-in *Luc* mice respond to changes in day length similar to endogenous photoperiodic genes in the PT. *TSH*β, *Luc* and *Cga* expressions in the PT of wild-type and heterozygous *TSH*β^{Luc} mice under different day-length conditions were analyzed by radioisotope (RI) *in situ* hybridization. After 3 weeks of exposure to short-day [light/dark = 8:16 hour (L8 : D16), zeitgeber time 0 (ZT0; ZT0 was defined as the time of lights-on) = lights-on, ZT8 = lights-off] or long-day (L16 : D8, ZT0 = lights-on, ZT16 = lights-off) conditions, brain samples from each light condition were collected 4 h before lights-off that corresponds to the same circadian phase under both conditions (Masumoto *et al.* 2010) (Fig. 2A). *TSH*β, *Luc* and *Cga* were detected only in the PT under both conditions, and the *TSH*β expression increased 2.5-fold under long-day conditions in wild-type and heterozygous *TSH*β^{Luc} mice. Although *Luc* expression was almost undetectable in heterozygous *TSH*β^{Luc} mice under short-day conditions and not detected in wild-type mice, its expression was clearly detected in heterozygous *TSH*β^{Luc} mice under long-day conditions (Fig. 2B). I also observed that *Cga* expression pattern was comparable in wild-type and heterozygous *TSH*β^{Luc} mice. These results indicate that the *Luc* expression represents the physiological photoperiodic responses of *TSH*β in the PT and does not affect the expressions of endogenous *TSH*β and *Cga*.

PT-specific signals of the TSHβ-Luc reporter

To detect bioluminescence derived from the *TSH*β promoter in the PT region, I prepared brain slices including regions from *TSH*β^{Luc} mice. First, I monitored the spatial pattern of the bioluminescence activity in the slice with a macrozoom microscope and a CCD camera. As expected, bioluminescence activity was observed only in the putative PT region surrounding the median eminence of the slices from 5- to 6-week-old (adult) heterozygous *TSH*β^{Luc} mice kept under long-day conditions for 2–3 weeks (Fig. 2C). These spatial bioluminescence patterns are compatible to signals of *Luc* mRNA (Fig. 2B,C). By contrast, no bioluminescence was observed in the slices from wild-type mice (Fig. 2C). Therefore, bioluminescence activity measured in the slice can be attributed to luc activity in the PT. In addition, similar bioluminescence pattern in the slices from adult mice was observed in the slices from postnatal 6- to 8-day-old (neonate) heterozygous *TSH*β^{Luc} mice kept under L12 : D12 (ZT0 = lights-on, ZT12 = lights-off) conditions (Fig. 2C). These observations are consistent with the *TSH*β expression *in vivo* (Schulze-Bonhage & Wittkowski 1990; Japon *et al.* 1994) and thus imply the possibility of slice usage from both adult and neonatal PT.

Real-time bioluminescence monitoring of the TSHβ-Luc reporter

Next, I developed a real-time monitoring system for *TSH*β-Luc bioluminescence by a photomultiplier tube (PMT). Because Luc appears to be specifically expressed in the PT of the slice (Fig. 2C), photon counts by PMT measurements represent a mean bioluminescence of the tissue. First, the bioluminescence signals of slices from adult heterozygous *TSH*β^{Luc} mice kept under short- or long-day conditions for 2–3 weeks (adult short- or long-day slices) were measured (Fig. 3A,B). Significantly higher bioluminescence signals were detected from adult long-day slices than from adult short-day slices and wild-type slices. I further checked whether the slices have *in vivo*-like responsiveness to photoperiodic signals. I treated adult long-day slices with 10 nM of melatonin from subjective ZT16 (ZT16 is the start of the culture and subjective night) (Fig. 3C). In agreement with previous *in vivo* studies (Ono *et al.* 2008; Unfried *et al.* 2009; Yasuo *et al.* 2010), a decrease in luc activity was observed by melatonin treatment. These results suggest that the experimental system keeps *TSH*β response to melatonin even in my culture condition.

One important application of this real-time monitoring system is to screen molecules that convey light signals under long-day conditions and induce the *TSH*β expression. Thus, I examined the possibility of using of neonatal tissues instead of adult tissues because of some advantages: (i) higher viability of tissues, (ii) ease of slice preparation and (iii) significant signal levels even in L12 : D12 conditioned animals rather than long-day conditioned animals (Fig. 2C). To check whether neonatal tissues can be used for the monitoring assay, luc activity in the PT slices of neonatal heterozygous *TSH*β^{Luc} mice kept under L12 : D12 conditions (neonatal slices) was measured (Fig. 3A). The robust bioluminescence activities of the neonatal slices were observed for over 2 days and gradually reached baseline levels after additional 2 or 3 days (Fig. 3D), with dynamics similar to those in adult long-day slices. Continuous luminescence in the PT for 2–4 days by imaging neonatal slices again confirmed that whole-tissue bioluminescence approximates activity in the PT (Fig. 4). Luminescence was also observed in individual PT cells over 4 days, but with noisy fluctuations (Fig. 4B). Furthermore, the neonatal slices were treated with various concentrations of melatonin, and dose-dependent repression was observed (Fig. 3E). These patterns of bioluminescence with or without melatonin were similar to the results in the adult long-day slices and *in vivo*.

To independently confirm that the observed dynamics of bioluminescence is correlated with endogenous *TSH*β expressions in neonatal PT slices, the expression levels of *TSH*β, *Eya3* and *Cga*, which are known to be decreased by melatonin (Ono *et al.* 2008; Unfried *et al.* 2009; Dardente *et al.* 2010; Yasuo *et al.* 2010), were measured by qPCR. Cultured PT tissues with vehicle or 10 nM of melatonin treatment for 48 h after the start of the culture were collected and subjected to qPCR analysis. The values of *sine*

oculis–related homeobox 5 (*Six5*) and *potassium voltagegated channel, subfamily Q, member 5* (*Kcnq5*) were used for measuring the relative PT amounts of the samples and normalizing *TSH*β values and related genes, because *Six5* and *Kcnq5* expression is specific to the PT and does not respond to melatonin (Dupre *et al.* 2008; Masumoto *et al.* 2010). Consistent with *in vivo* observations (Ono *et al.* 2008; Unfried *et al.* 2009; Dardente *et al.* 2010; Yasuo *et al.* 2010) and bioluminescence results, the expression levels of endogenous *TSH*β, *Eya3* and *Cga* were significantly decreased under melatonin treatment, excluding the possibility that the decrease in the bioluminescence by melatonin might be an artifact (Fig. 3E,F). In addition, there was a strong positive correlation between *TSH*β mRNA levels by qPCR analysis and bioluminescence counts of the PT slices by PMT measurements (r^2 = 0.71; Fig. 3F, right). Furthermore, the culture medium of neonatal PT slices in Fig. 3F was collected, and secreted TSHβ amounts were measured by mass spectrometry. In the melatonin-treated culture medium, secreted TSHβ amounts were 50% lower than vehicle-treated samples (Fig. 3G). There was a strong correlation between secreted TSHβ amounts and the bioluminescence counts (r^2 = 0.81; Fig. 3G, middle) as well as the *TSH*β mRNA levels (r^2 = 0.66; Fig. 3G, right). These results indicate that the responsiveness of the luc activity to an external signal reflects *TSH*β mRNA expression and secreted TSHβ protein.

Recently, it was reported that glutamine and glutamic acid induce the *TSH*β expression in the rat PT (Aizawa *et al.* 2012). To check whether the mouse PT also responds to glutamine and glutamic acid, the slices were treated with 1 mM of glutamine or 1 mM of glutamic acid after 2 h of glutamine and glutamic acid starvation. Although no response was observed by glutamine treatment, a transient increase in luc activity was observed by glutamic acid treatment. These results suggest that the slices can also respond to an inducer of *TSH*β (Fig. 5).

In summary, I visualized the *TSH*β expression dynamics in the PT by using adult and neonatal *TSH*β^{Luc} mice and observed responsiveness of the *TSH*β expression to an external signal.

2. Screening of candidate TSHβ upstream molecules by using TSHβ real-time monitoring system

Screening of candidate TSHβ upstream molecules; intracellular signal transduction

To identify upstream molecules of *TSH*β mimicking light stimulation, I first screened the effects of drugs which perturb a candidate *TSH*β-regulating pathway in the PT cells by using my real-time monitoring system. First, I focused on cAMP pathway mediated by G-protein coupled receptors (GPCRs). Previous studies have shown that the PT expresses the pertussis toxin (PTX)-sensitive MT1 GPCR. Because PTX is a molecule that catalyses the ADP-ribosylation of G_i family G-protein and prevents the occurrence of the receptor-G_i interaction (Mangmool & Kurose 2011), MT1 is thought to be the receptor coupling with G_i and suppress the intracellular cAMP levels. Given that *TSH*β is suppressed by melatonin-MT1

pathway, the suppression is possibly mediated through the G_i-induced cAMP downregulation. Thus, I hypothesized that the elevation of intracellular levels of cAMP inversely induces *TSH*β. To explore this possibility, I tested the effects of forskolin, an adenylate cyclase (AC) activator, on the luc signal levels in the PT slices. Here I tested three timing of the drug addition. First, I added the drug at the start of the culture. In the condition with the drug, 12 h delay of the following increase in luc activity after the treatment and more gradual increase in luc activity were observed compared with vehicle treatment (Fig. 6A). Furthermore, whereas vehicle-treated slices showed two distinct peaks of luc activity (1st peak after 26 h and 2nd peak after 44 h from starting the culture), forskolin-treated slices showed a single peak after 56 h from starting the culture (Fig. 6A). However, no further increase of luc signals were observed. To mimic the *in vivo* condition for *TSH*β induction more precisely, I next tried the 8 h-advanced lights-on condition (light-on 8 h after light-off), which is reported as the experimental condition of long-day stimulation in CBA/N mice (Fig. G5) (Masumoto *et al.* 2010). Because I started the culture at the timing of light-off (subjective ZT12), the drug were added 8 h or 8+24 h after the start of the culture. When forskolin was added 8 h after the start of the culture, luc activity was transiently decreased to significantly lower levels during the following 11 h after the drug treatment, and it eventually recovers as same level as vehicle treatment after 68 h from the treatment (Fig. 6B). Moreover, when forskolin was added 8+24 h after the start of the culture, luc activity was temporarily decreased to 0.3-fold during the following 11 h from the drug treatment, and then increased to 1.2-fold 40 h after the treatment compared with vehicle (Fig. 6C). Interestingly, these three experiments showed that the following increase in luc activity after forskolin treatment delays for approximately 12 h after the treatment. Furthermore, the second and third experiments showed the unexpected transient decrease. To rule out the possibility that competition for ATP between activated AC by forskolin and bioluminescence reaction of luciferase caused the transient decrease in apparent bioluminescence, I decided to use chemicals that stimulate downstream molecules of cAMP. Thus I treated the PT slices with a protein kinase A (PKA) selective agonist, 6-Bnz-cAMP (PKA agonist) or an exchange protein directly activated by cAMP (Epac) selective agonist, 8-pCPT-2'-*O*-Me-cAMP (Epac agonist), both of which act downstream of the cAMP signal. 500 μM or 2.5 mM of the PKA agonist induced continuous increase in luc activity compared with vehicle treatment and finally reached to the higher levels than vehicle treatment. Furthermore, 500 μM of Epac agonist increased luc activity to 1.5-fold 54 h after the treatment compared with vehicle treatment with some delayed peak (5 h delay from the peak in vehicle condition), although 100 μM of the compound had no significant effect (Fig. 6D). Taken together, I perturbed PKA or Epac signal to avoid possible competition for ATP, and a gradual increase in luc activity was observed by the treatment. The increased luc activity by 500 μM or 2.5 mM of the PKA agonist, or 500 μM of the Epac agonist treatment became higher than

that by vehicle treatment approximately 1.5, 2.5, or 2 days after the treatment, respectively (Fig. 6D). Forskolin treatment 8+24 h after the start of the culture also increased luc activity higher than vehicle treatment 28.5 h after the treatment (Fig. 6C). However, time-scale of induction of luc activity by these treatments is longer than that of *TSH*β by long-day stimulation. Because long-day stimulation increased *TSH*β expression level gradually for 8-12 h *in vivo* (Masumoto *et al.* 2010), these results suggest that AC-PKA pathway and AC-Epac pathway are not likely to be involved in acute *TSH*β induction by long-day stimulation. On the other hand, the delay of increase in luc activity after the treatment was not observed by the PKA agonist or the Epac agonist treatment, in contrast to forskolin treatment, implying that PKA or Epac is not involved in the phenomenon (Fig. 6A-D). It is still unclear that why a transient decrease in luc activity was observed only by forskolin treatment (Fig. 6B and 6C).

To further check the role of the cAMP signal in *TSH*β expression I treated the PT slices with MDL-12,330A (MDL), a potent, irreversible inhibitor of AC, from the start of the culture. 1 μM or 10 μM of MDL treatment reduced (0.7-fold) or completely inhibited the increase of luc activity during the experiment, suggesting that pharmacological inactivation of AC suppressed *TSH*β promoter activity (Fig. 6E). This observation is consistent to the considering mechanism of *TSH*β reduction by melatonin-MT1-AC inhibition pathway. However, the possibility of tissue damage by the reagent should be also ruled out with an additional experiment such as measuring some endogenous genes by qPCR.

Although it seemed reasonable to hypothesize that *TSH*β induction starts immediately after cAMP elevation, I could not find that any cAMP signal-related drugs inducing luc activity in compatible to the time-scale *in vivo*. To consider the signal hypothesis again, I next checked whether suppression of luc activity by melatonin treatment is PTX dependent as reported (Morgan *et al.* 1990). 1 μg / mL of PTX was added with 10 μM of melatonin 8+24 h after the start of the culture. Unexpectedly, a 1.3-fold increase in luc activity was observed 6.5-8 h after the treatment compared with vehicle of melatonin treatment (Fig. 6F). An increase in luc activity was also observed by melatonin and PTX treatment, suggesting that PTX treatment is unlikely to cancel the melatonin effects on luc activity. Furthermore, melatonin treatment 8+24 h after the start of the culture did not suppress luc activity. Note that because the experiment was preliminarily performed using n = 1 sample, the result should be carefully interpreted considering its reproducibility. To further evaluate PTX dependency of melatonin-MT1-*TSH*β pathway, the similar experiments should be performed under *TSH*β-suppressing condition by melatonin treatment from the start of the culture.

I also tested the possible involvement of protein kinase C (PKC), phospolipase C (PLC), calcium ion, and potassium ion as *TSH*β upstream cascades. 12-*O*-tetradecanoyl phorbol 13-acetate (TPA), a PKC activator, was added to PT slices 8+48 h after the start of the culture. 0.2 μM of TPA had no effects, and

2 μM of TPA slightly decreased luc activity. 20 μM of TPA decreased luc activity to 0.7-fold, compared with vehicle treatment (Fig. 7A). M-3M3FBS, a PLC activator, had also no effect when the chemical was added 8+48 h after the start of the culture (Fig. 7B). Treatment with a calcium ionophore ionomycin for 30 min significantly decreased luc activity to 0.3-fold, compared with vehicle treatment (Fig. 7C). 10 mM of KCl treatment from the start of the culture decreased luc activity to 0.5-fold, compared with vehicle treatment. Further increase of KCl concentration to 60 mM, luc activity became to be significantly noisy (Fig. 7D). A decrease in luc activity by TPA, ionomycin and KCl treatment might be due to suppression of *TSH*β promoter activity, or these treatments simply damaged to PT slices (Fig. 7A, C and D). Thus, additional experiments will be needed to distinguish these possibilities.

In summary, I performed several screening of candidate drugs targeting for cAMP signaling, PKC, PLC, calcium ion, and potassium ion. There was no drug that can induce *TSH*β immediately after the treatment as in *in vivo* light stimulation.

Screening of candidate TSHβ upstream molecules; extracellular signal transduction

For the next screening, I focused on molecules existing outside of PT cells. First, I checked whether *TSH*β is fully induced only by removal of melatonin because (1) melatonin suppresses *TSH*β, and (2) light pulse for 15 min decreased melatonin level within 45 min and melatonin is not secreted during daytime *in vivo* (Kennaway *et al.* 2002). 10 pM of melatonin was added to PT slices from the start of the culture, and was removed by medium changing after 8, 16, 24 h from starting the culture. However, luc activity was not recovered by the removal of melatonin at any timings (Fig. 8A). These observations suggest that only melatonin removal is not sufficient for *TSH*β induction and thus additional molecules appears to be needed.

Then I moved to search such additional molecules. First, I focused on serotonin because concentration of the molecule shows seasonal variation in the brain (Lambert *et al.* 2002). To determine whether the PT expresses any types of serotonin receptor subtypes, RI *in situ* hybridization was performed. Some of the serotonin receptor subtypes such as *Htr1b*, *Htr3a*, *Htr5a*, and *Htr6* were expressed in the PT (Fig. 9A). Next, I checked whether serotonin induces *TSH*β by using the *TSH*β real-time monitoring system. PT slices were treated with 5, 10 or 30 μM of serotonin 8+24 h after the start of the culture. Two distinct peaks (2 and 13 h after serotonin treatment) of luc activity were observed and both peaks showed a 1.2-1.3-fold increase compared with vehicle treatment (Fig. 9B). One concern is that the intrinsic fluorescence of serotonin is detected by PMT, because it is known that tryptophan, a precursor of serotonin, has a fluorescence property. To rule out this possibility, I assessed the effects of the intrinsic fluorescence of serotonin in this real-time monitoring system. Indeed, serotonin treatment increased raw

photon counts in a dose-dependent manner. 10 μM and 30 μM of serotonin addition to neonatal PT slices from CD-1 mice that do not carry luc reporter increased raw photon counts to 1.25-fold and 1.5-fold, respectively (Fig. 9C). These results suggest that the intrinsic fluorescence of serotonin can be detected by PMT and distinguishing between the serotonin's intrinsic fluorescence and an increase in luc activity by serotonin treatment is difficult. To further analyze the serotonin effects on *TSH*β expression, I examined whether serotonin induces *TSH*β in the PT *in vivo*. 3-week-old CBA/N mice kept under short-day conditions were chronically administrated fluoxetine (10 or 22 mg/kg/day) or paroxetine (10 or 30 mg/kg/day), two representative selective serotonin reuptake inhibitors (SSRIs), for 2 weeks. I evaluated the effects of SSRIs on *TSH*β expression levels in the PT by RI *in situ* hybridization, and I did not find any significant difference (Fig. 9D). These results indicate that serotonin is not likely to have a role on *TSH*β induction.

Next, I focused on GPCRs expressed specifically in the PT region. I hypothesized that some GPCRs competing with MT1 might induce *TSH*β. Here I screened for candidate GPCRs expressed in the median eminence (ME) region including the PT from Brainstars, a quantitative expression database of the adult mouse brain including genome-wide expression profile at 51 adult mouse central nervous system regions (Kasukawa *et al.* 2011). TSH receptor (*Tshr*), *sphingosine-1-phosphate receptor-3* (*S1pr3*), *cysteinyl-leukotriene type-1 receptor* (*Cysltr1*), and *frizzled-5* (*Fzd5*) were picked up as candidate GPCRs. In addition, MT1 (*Mtnr1a*) was also picked up by this screening, suggesting that this screening is functional for picking up candidate GPCRs in the PT. Expression patterns of these candidate genes were analyzed by RI *in situ* hybridization, and *Mtnr1a*, *Tshr*, and *Fzd5* were indeed expressed in the PT (Fig. 10A), consistent with previous studies reporting that *Mtnr1a* and *Tshr* were expressed in the mouse PT (Roca *et al.* 1996; Ono *et al.* 2008; Unfried *et al.* 2009). In contrast, *S1pr3* and *Cysltr1* expression were not detected in the PT (Fig. 10A). Thus, I tested the possibility of positive feedback by *TSH*β itself. PT slices were treated with 1 or 10 mIU/mL of TSH from the start of the culture, but no effect on luc activity was observed (Fig. 10B).

An output molecule from the SCN that controls circadian clock was also examined because photoperiodism is based on circadian rhythms. *Prokineticin 2* (*Pk2*) is reported as output molecule of the SCN, and administration of PK2 altered wheel-running activity in rats (Cheng *et al.* 2002). 20 nM of recombinant PK2 treatment 8+48 h after the start of the culture did not alter luc activity in PT slices (Fig. 11A). Furthermore, *prokineticin receptor 2* (*Pkr2*) was not expressed in the PT (Fig. 11B). These results indicate that PK2-PKR2 pathway is unlikely to be involved in *TSH*β induction.

Glutamic acid, one of excitatory neurotransmitters, is a candidate upstream molecule of *TSH*β-inducible signals. It was reported that glutamic acid induces the *TSH*β expression in the rat PT (Aizawa *et al.* 2012).

Furthermore, a transient increase in luc activity was observed by glutamic acid treatment by using *TSH*β real-time monitoring system (Fig. 5). Therefore, I tested whether glutamic acid receptor agonists can induce *TSH*β. PT slices were treated with 50 μM of kainic acid (KA), 50 μM of alpha-amino-3-hydroxy-5-methyl-4-isoxazolepropionic acid (AMPA), or 50 μM of N-methyl-D-aspartic acid (NMDA) after 2 h of glutamine and glutamic acid starvation, resulting in no changes in luc activity were observed (Fig. 12).

Taken together, among candidate extracellular molecules for which I performed screening in this study, I did not find any *TSH*β-inducible signals except glutamic acid.

3. Analysis of time dependency in TSHβ induction by using TSHβ real-time monitoring system

Analysis of time dependency in luc activity in response to melatonin removal and forskolin treatment

It is believed that light stimuli at specific time can induce photopeperiodic responses (gating mechanism) because photoperiodism is based on circadian clock (Bünning 1936; Ravault & Ortavant 1997). Our group previously showed that light stimulation at the subjective late night can rapidly induce *TSH*β in the mouse PT, suggesting that the timing of light stimulation is important for *TSH*β induction (Masumoto *et al.* 2010). Thus, I examined whether *TSH*β is induced by the treatment at a specific timing. First, I hypothesized that a decrease in melatonin levels by light stimulation at a specific time induces *TSH*β. However, three different timings of melatonin removal did not alter luc activity of PT slices (Fig. 8A). To check the possibility that not only melatonin removal but also another stimulation is necessary for *TSH*β induction, melatonin was removed and forskolin was applied to PT slice. PT slices were treated with 10 pM of melatonin from the start of the culture and melatonin was removed 8, 16, and 24 h after the start of the culture. At the same time, 1 μM of forskolin was applied to PT slices. These treatments decreased luc activity transiently for approximately 12 h after treatments and a following increase in luc activity was observed. (Fig. 8B). Removal of melatonin with/without forskolin treatment did not induce luc activity immediately after the treatment. These observations suggest that *TSH*β response to melatonin removal and forskolin does not have time-dependency in this experimental condition.

Discussion

In the present study, I established a *TSH*β real-time monitoring system in which the *TSH*β expression dynamics can be monitored as real-time bioluminescence activities. The difference in luc activity of PT slices derived from adult mice under short- or long-day conditions was consistent with *in vivo TSH*β expression levels in response to each day-length condition (Fig. 2, 3B). Moreover, the luc activities of adult and neonatal PT slices were suppressed by melatonin treatment (Fig. 3C,E). I also observed dose-dependent suppression of *TSH*β in neonatal PT slices by melatonin (Fig. 3E) at physiological levels (Kennaway *et al.* 2002), which is consistent with the results using ovine PT cell cultures (Morgan *et al.* 1989). Furthermore, the luc activities were transiently up-regulated by glutamic acid treatment as seen in the rat PT (Aizawa *et al.* 2012) (Fig. 5). These observations suggest that PT slices possess at least *TSH*β responsiveness to melatonin and glutamic acid, and changes in *TSH*β expression dynamics under other stimuli are also expected to be observed by using my monitoring system. Furthermore, I performed preliminary screening for candidate upstream molecules of *TSH*β, however, I did not find any intracellular or extracellular molecules that upregulate luc activity except glutamic acid in this study.

Chronic melatonin treatment in this monitoring system may not necessarily the same as physiological conditions, comparing with nocturnal melatonin secretion *in vivo*. However, because *TSH*β was induced within several hours after long-day stimulation *in vivo*, this monitoring system is at least available for screening of candidate molecules upstream of *TSH*β, by observing luc activity during the same period. Transiently increased luc activity by glutamic acid treatment supports this idea (Fig. 5).

Some observations and experimental conditions were not consistent with *in vivo* conditions. First, several studies show that melatonin implantation (constant release of melatonin) has no effect on testicular regression in hamsters (Goldman *et al.* 1979). Furthermore, melatonin injection under long-day conditions does not suppress *TSH*β expression for at least 4 days in hamster (Yasuo *et al.* 2010), which is inconsistent with the immediate suppression presented in Fig. 3C. I speculate that difference between these *in vivo* observations and my *in vitro* results may be due to experimental conditions such as existence of *TSH*β-inducible signals. Second, melatonin decreased luc activity and the activity was not recovered for the following 2-3 days after melatonin removal (Fig. 8A). Melatonin is lipophilic, implying that it is almost impossible to remove them completely by medium changing. Melatonin may be remained in the PT slices after medium changing. Furthermore, Cytochrome P450 1A2 (CYP1A2), which degrades melatonin in the liver, seems not be exist in PT slices because *Cyp1a2* is not expressed in the ME region (Kasukawa *et al.* 2011; Choudhary *et al.* 2011). Third, I added drugs to PT slices without following removal of drugs except ionomycin treatment (Fig. 7C). Although a drug treatment for a long time is

different form physiological conditions, a transient drug treatment such as ionomycin treatment will more precisely mimic *in vivo* conditions. Fourth, I observed a significant decrease in luc activity for approximately 12 h after the start of the culture. One possibility is that the PT clock was reset by PT slice preparation. Another possibility is that *TSH*β-inducible signals *in vivo* were lost by preparation. Measuring some endogenous expressions of circadian clock genes by qPCR will reveal the effect of slice preparation on the PT clock. Therefore, careful design of experiments will be necessary in each purpose.

One possible application of my experimental system is to screen upstream light information signals of the *TSH*β induction. My system has several advantages for this purpose: (i) The PT slices can be used and easily treated with drugs compared with previous methods such as subcutaneous injection (Yasuo *et al.* 2007), intracerebroventricular injection (Ono *et al.* 2008) or dissociated PT cells (Morgan *et al.* 1989), (ii) availability of neonatal tissues increases the throughput of the experiment and viability of the slices. Previous reports support that neonatal PT has the similar photoperiodic properties to adult PT. First, high expression levels of *TSH*β (Schulze-Bonhage & Wittkowski 1990; Japon *et al.* 1994), MT1 receptor (Williams *et al.* 1991; Johnston *et al.* 2003) and rhythmic expression of the clockwork genes (Ansari *et al.* 2009) were observed in both embryonic and neonatal PT. Second, fetal and neonatal lambs showed changes in prolactin concentration in response to day-length (Ebling *et al.* 1988; Ebling *et al.* 1989).

I performed screening for candidate upstream molecules of *TSH*β. Cyclic AMP was a candidate *TSH*β-inducible molecule because MT1 is reported to be G_i-coupled receptor. Forskolin, PKA agonist, or Epac agonist treatment increased luc activity more gradually compared with vehicle treatment, and time-scale of induction was inconsistent with the case of light stimuli *in vivo* (Fig. 6A-D). An increase in luc activity by cAMP elevation had been initially expected to start immediately after the treatment because light pulse for 15 min suppresses pineal melatonin and plasma melatonin concentrations to basal levels within 45 min from the start of light exposure (Kennaway *et al.* 2002). Thus, the inconsistency suggests that cAMP signal is not likely to be involved in acute *TSH*β induction. On the other hand, it is reported that *TSH*β expression level under long-day conditions for 2 weeks was higher than that in the first long-day (Masumoto *et al.* 2010). Thus, cAMP signaling may be involved in a gradual increase and/or maintenance of *TSH*β expression after acute induction of *TSH*β by long-day stimulation. Unexpectedly, forskolin treatment during the culture caused a transient decrease in luc activity (Fig. 6B and C). One interpretation for the phenomenon is that competition for ATP between activated AC by forskolin and bioluminescence reaction of luciferase caused the transient decrease in apparent bioluminescence. Another interpretation is that a transient decrease in luc activity may due to acute induction of negative regulators by forskolin treatment. For example, it is reported that forskolin induced *Per1* immediately in fibroblasts (Balsalobre *et al.* 2000; Yagita & Okamura 2000) and *Per1* reduced the

Bmal1-*Clock*-induced *TSH*β promoter activity in *in vitro TSH*β promoter assay (Unfried *et al.* 2009). On the other hand, forskolin treatment at the start of the culture just delayed the increase in luc activity and did not decrease it compared with vehicle treatment (Fig. 6A). The decrease in luc activity by forskolin treatment at this timing may be masked because the significant decrease in luc activity for first 12 h was also observed by vehicle treatment. Furthermore, the observed delay of the increase in luc activity may possibly be due to resetting of the PT clock by forskolin treatment. Several previous reports support this idea. First, forskolin resets expression patterns of circadian clock genes in various tissues including the SCN (Prosser & Gillette 1989; Yagita & Okamura 2000; Abe *et al.* 2002; Izumo *et al.* 2006). Second, circadian clock genes or PER2::LUC monitoring molecule are expressed and oscillating in the PT or the median eminence/pars tuberalis region, respectively (Ansari *et al.* 2009; Guilding *et al.* 2009; Masumoto *et al.* 2010). Third, some reports indicate that circadian clock genes control *TSH*β expression in *in vitro TSH*β promoter assay (Unfried *et al.* 2009; Masumoto *et al.* 2010). To further check whether forskolin reset the PT clock in future studies, a possible way is monitoring the spatial pattern of the bioluminescence activity in PT slices from PER2::LUC knock-in mice with a macrozoom microscope and a CCD camera (Yoo *et al.* 2004), with or without forskolin treatment. Interestingly, PKA agonist or Epac agonist treatment that act downstream of AC did not cause the delay of increase in luc activity after the treatment (Fig. 6D), suggesting that the observed delay is possibly due to AC activation. Furthermore, whether melatonin-MT1-*TSH*β pathway is mediated by the G_i-coupled receptor and antagonizes the cAMP signal should be checked carefully. When melatonin was added to the PT slices with a G_i inhibitor PTX, the pattern of luc activity by melatonin treatment was not canceled (Fig. 6F). To further explore the possibility of cAMP involvement in *TSH*β induction, I think it is necessary to observe the response of the signal to day-length change *in vivo*. I also performed experiments about other signaling pathway such as PKC, PLC, calcium ion, and potassium ion to screen candidate *TSH*β upstream cascades, any upregulator of luc activity was not found in this study (Fig. 7). Other drug treatments that act different action points and identification of the detailed signaling of melatonin-MT1-*TSH*β pathway are important in future. One candidate signaling involved in melatonin-MT1-*TSH*β pathway is the $G_{q/11}$ pathway. It is reported that human MT1 functionally couples with G_i and $G_{q/11}$ proteins by coprecipitation experiments (Brydon *et al.* 1999). Treating the PT slices with melatonin and YM254890, a $G_{q/11}$ inhibitor, will reveal whether melatonin-MT1-*TSH*β pathway is dependent on the $G_{q/11}$ pathway. Moreover, other drugs targeting the $G_{q/11}$ pathway such as U73122 (a PLC inhibitor), bryostatin 1 (a PKC activator), and C-1 (a PKC inhibitor) will help to reveal a role of the $G_{q/11}$ pathway on *TSH*β induction. Meanwhile, because melatonin removal from the PT slice culture medium did not alter luc activity suppressed by melatonin, other *TSH*β-inducible signals seem to highly exist (Fig. 8A). The screening of candidate *TSH*β upstream

molecules existing outside of the PT cells was performed. First, I tested the effects of serotonin that shows seasonal variation in the brain. Although some of serotonin receptor subtypes were expressed in the PT, serotonin administration did not alter *TSH*β *in vivo* (Fig. 9A and D). Second, I focused on GPCRs expressed specifically in the PT region and possibly competing with MT1. I confirmed that *Mtnr1a*, *Tshr*, and *Fzd5* were expressed in the PT. However, TSH did not increase luc activity (Fig. 10). Other candidate GPCR was *Fzd5*, the receptor for *Wnt5a* ligand (Tanaka *et al.* 1998; Ishikawa *et al.* 2001). The involvement of Wnt5a-Fzd5 pathway in *TSH*β induction should be examined in the future. Third, PK2, an output molecule from the SCN was examined because photoperiodism is based on circadian clock. However, *Pkr2*, the receptor of PK2, was not expressed in the PT and PK2 did not have any effects on luc activity (Fig. 11). Finally, I checked whether glutamic receptor agonists can induce *TSH*β because a transient increase in luc activity was observed by glutamic acid treatment (Fig. 5). However, KA, AMPA, or NMDA did not alter luc activity (Fig. 12). Collectively, I could not find any *TSH*β-inducible signals except glutamic acid. These results suggest that glutamic acid is one of *TSH*β-inducible signals. Note that glutamic acid induces luc activity weakly, implying that other *TSH*β-inducible signals are necessary for efficient induction of *TSH*β. For example, *transforming growth factor alpha* (TGFα), *cardiotrophin-like cytokine* (CLC), and *vasoactive intestinal peptide* (VIP), which are reported as output molecule of the SCN and alter circadian rhythms of behavior or hormone (Harney *et al.* 1996; Kramer *et al.* 2001; Kraves & Weitz 2006), and neurotransmitters of avian deep brain photoreceptors are candidates of *TSH*β-inducible signals (Halford *et al.* 2009; Nakane *et al.* 2010; Yamashita *et al.* 2010). Unfortunately, neurotransmitters of avian deep brain photoreceptors have been unidentified yet. I hope neurotransmitters of avian deep brain photoreceptors will be identified because Opsin-5, one of deep brain photoreceptors, is suggested to be involved in *TSH*β induction in Japanese quails (Nakane *et al.* 2014). Furthermore, comprehensive analysis of gene expression patterns in the PT immediately after long-day stimulation will reveal acute response genes to long-day stimulation, and information of these genes may provide hints for candidate *TSH*β upstream molecules.

My system is also applicable to investigate the mechanism of photoinducible phase (gating), by which the response of the PT to a light signal including *TSH*β induction is gated during the late night (Masumoto *et al.* 2010). Internal circadian time is probably involved in the determination of the gate timing, because photoperiodic responses can be induced by light stimuli at specific time (Ravault & Ortavant 1997). Thus, I checked time-dependency of *TSH*β responsiveness by different timings of treatment such as melatonin removal and forskolin treatment (Fig. 8). Melatonin removal alone at different timings did not recover suppressed luc activity. Melatonin removal plus forskolin treatment at different timings decreased luc activity transiently and a following gradual increase was observed. These results imply that melatonin

removal and forskolin treatment are not likely to have time-dependency in *TSH*β responsiveness and forskolin may possibly reset the PT clock in this experimental condition. Treatment with a *TSH*β-inducible molecule that does not affect the PT clock is important to test for time-dependency of *TSH*β responsiveness. Besides, analysis of the relationship between circadian clock genes and *TSH*β will also provide hints for the gating mechanism. It is reported that several circadian clock genes and circadian clock-controlled genes regulate *TSH*β promoter activity by *in vitro TSH*β promoter assay (Unfried *et al.* 2009; Masumoto *et al.* 2010). Thus, similar experiments using the PT slices from mice generated by mating *TSH*β^{Luc} mice with knockout mice of circadian clock genes will help to reveal the detailed relationship between circadian clock genes and *TSH*β. Furthermore, it is also important to understand the molecular mechanism of the PT clock by using the PT slices from PER2::LUC knock-in mice, because rhythmic expression of circadian clock genes in the PT is melatonin-dependent and this property is different from the SCN clock.

The *TSH*β^{Luc} mice generated here are the first report of *TSH*β null mice. *TSH*β^{Luc} mice enabled us to study the photoperiodic roles of *TSH*β. Although *TSH*β is also expressed in the pituitary and functions as a part of the hypothalamus–pituitary–thyroid (HPT) axis, it is believed that the molecule in the PT acts differently from the HPT axis. This idea is supported by the results that *TSH*β expression in ovine PT did not change with thyroid-releasing hormone (TRH) and thyroid hormone (TH) treatment, because the lack of TRH and TH receptor or transcription factor *Pit-1* induces *TSH*β in the pituitary (Bockmann *et al.* 1997). Growth retardation observed in homozygous *TSH*β^{Luc} mice (Fig. 1D) is consistent with previous observations in hypothyroid mice, such as TSHR knockout mice (Marians *et al.* 2002), the Snell dwarf mice (Cordier *et al.* 1976), the cog mice (Taylor & Rowe 1987) and the hyt mice (Beamer *et al.* 1981), and could be recovered by supplementation with thyroid powder (Fig. 1D). Thus, photoperiodic phenotypes in the *TSH*β^{Luc} mice, if any, can be discriminated from the effects of the impaired HPT axis by supplementation with thyroid powder. Because no obvious photoperiodic phenotype has not been identified in laboratory mice, such as testicular growth, which is a typical photoperiodic phenotype (Ono *et al.* 2008), it will be intriguing to further explore photoperiodic phenotypes in laboratory mice with reference to known seasonal physiological changes such as gonad growth in female European hamsters (Hanon *et al.* 2010), metabolic changes such as adipose depot mass and serum leptin (Atcha *et al.* 2000) and immune system such as NK cell cytolytic activity and phagocytosis in Siberian hamsters (Yellon *et al.* 1999; Martin *et al.* 2008). Even if no obvious photoperiodic phenotype can be identified in laboratory mice, molecular mechanisms underlying the induction of *TSH*β by long-day light exposure are evolutionary conserved (Hanon *et al.* 2008; Nakao *et al.* 2008; Ono *et al.* 2008; Dardente *et al.* 2010; Dupre *et al.* 2010; Hanon *et al.* 2010; Masumoto *et al.* 2010; Yasuo *et al.* 2010). Therefore, *TSH*β^{Luc} mice,

established in this study, will provide useful insights into the evolutionary conserved molecular mechanism of photoperiodism.

Conclusion

In this thesis, I established an experimental system for screening candidate upstream molecules of *TSH*β. I generated a genetic mouse model in which *TSH*β expression dynamics in the PT can be visualized by bioluminescence. In the mouse strain, a part of coding sequence of *TSH*β was replaced by *Luc* gene and thus the luc activity represents direct transcription from the endogenous *TSH*β promoter. Animals were backcrossed and maintained on a CBA/N background and I found that phenotypes of heterozygous *TSH*β^{Luc} mice were comparable with those of wild-type mice, whereas homozygous *TSH*β^{Luc} mice showed growth retardation. I also confirmed that the *Luc* expression represented the physiological photoperiodic responses of *TSH*β in the PT and did not affect the expressions of endogenous *TSH*β and *Cga* by *in situ* hybridization of *TSH*β^{Luc} mice exposed to short-day or long-day conditions. I prepared brain slices including PT regions from *TSH*β^{Luc} mice and bioluminescence activity was observed only in the putative PT region. Treatment of cultured PT slices with melatonin decreased bioluminescence activities, endogenous *TSH*β expression and secreted TSH protein in the cultured medium. These results showed that PT slices can response to melatonin in our culture condition. Thus, my mouse model could be used to search for molecules that relay external light signals in the PT. Furthermore, I performed preliminary screening for candidate upstream molecules of *TSH*β such as drugs targeting the intracellular signaling pathways, hormones, and so on, and I found that glutamic acid is a strong candidate of *TSH*β-inducible molecules in this study. Unexpectedly, activators of cAMP-related molecules did not increase bioluminescence activities immediately after the treatment as seen in *TSH*β induction *in vivo*. Identification of upstream molecules of *TSH*β is one of the next attractive issues. I hope the knowledge obtained in this study will provide the clues to comprehend the mechanism for day-length measurements in mammalian photoperiodism.

Experimental procedures

Generation of TSHβ^{Luc} mice

*TSH*β^{Luc} mice [Tshb(Luc); Acc. No. CDB0713K: http://www.cdb.riken.jp/arg/mutant%20mice%20list.html] were generated as follows: a 1.9 kbp of Luc cassette that contains *Luciferase* (*Luc*)-coding region and simian virus 40 polyadenylation signal was amplified by PCR from pGL4.10 (Promega, Madison, WI, USA) using Luc-F-EcoRI (5′-AGAATTCTACTGTTGGTAAAGCCACCATGGAAGAT-3′) and Luc-R-NotI (5′-CGGAGCGGCCGCGATTTTACCACATTTGTAGAGGTTTTACTTGC- 3′) primers (Hokkaido System Science, Sapporo, Japan). The amplified product was ligated into the EcoRI/NotI site of pBluescript SK (−) (Stratagene, La Jolla, CA, USA). The 6.3-kb 5′-arm was PCR-amplified from a bacterial artificial chromosome (BAC) clone containing *TSH*β (RP24-230F23; BACPAC Resources, Oakland, CA, USA) using 5-F-SalI (5′-GCAGGTCGACCAATAGAGGGAACAGAATAGTCCCAAACG- 3′) and 5-R-BsmBI (5′-ACGGCGTCTCTCATGCTGAATCAGAGAGAAACATCAAAGAGCTC-3′) primers, and the amplicon was ligated into the SalI/ NcoI site upstream of the Luc of pBluescript SK (−) to make the 5′ arm-Luc cassette, in which the Luc cassette was connected in frame to the first ATG of the *TSH*β gene. The 5′ arm-Luc cassette was inserted into the SalI/NotI site of the PGK-Neo-pA/DT-A vector (detailed descriptions of the vector are available from http://www.cdb.riken.go.jp/arg/cassette. html). The 2.8-kbp 3′-arm was also PCR-amplified from the BAC clone using 3-F-AvrII (5′-GACCCTAGGATGTTGTTCAATGCATTTCTTTTAGCTGTAA-3′) and 3-R-SalI (5′-ATTAGTCGACGTACCATGCTATGCTGTTAACCTGCAATAC-3′) primers, and the amplicon was ligated into the XbaI/XhoI site of the PGK-Neo-pA/DT-A vector. The resultant targeting vector was linearized with the AscI site and introduced into TT2 embryonic stem cells by electroporation (Yagi *et al.* 1993; Murata *et al.* 2004). Screening of homologous recombinant embryonic stem cells and production of chimera mice are described elsewhere (http://www.cdb.riken.jp/arg/Methods.html). PCR primers used to routinely identify the wild-type allele are P1 (5′-CGCAGGGCCCAGGGATAAGTAACCAGTCAG-3′) and P2 (5′-ACCCGTGTCATACAATACCCAGCACAGATGGTG-3′); those to identify the mutant allele are P1 (5′-CGCAGGGCCCAGGGATAAGTAACCAGTCAG-3′) and P3 (5′-ACAGCCACACCGATGAACAGGGCACCCAAC-3′) (Fig. 1A). PCR products of 305 and 446 bp were derived from wild-type and mutant alleles, respectively. For Southern blot analysis, genomic DNA extracted from ES cells or a mouse tail was digested with AvrII, and resulted bands were detected with radioactive probes (14.5- and 18-kbp bands from wild-type and mutant alleles, respectively, in Fig. 1A).

Many laboratory mouse strains such as C57BL/6 lack melatonin production ability because of natural knockdown of the serotonin N-acetyltransferase (AANAT) activity (Roseboom *et al.* 1998) and low expression levels of hydroxyindole *O*-methyltransferase (HIOMT) protein (Kasahara *et al.* 2010; Shimomura *et al.* 2010), which are rate-limiting enzymes for melatonin synthesis. By contrast, CBA/N mice are melatonin proficient and they show significant *TSH*β induction after long-day stimulation (Ono *et al.* 2008; Masumoto *et al.* 2010). Thus, *TSH*β^{Luc} mice were backcrossed for more than 10 generations and maintained on a CBA/N background for all experiments except the measurement of growth in Fig. 1D (more than four generations).

Animals

Mice were carefully kept and handled according to the RIKEN Regulations for Animal Experiments. For *in situ* hybridization experiments, L12 : D12 conditioned male 3-week-old wild-type and heterozygous *TSH*β^{Luc} mice were housed under short-day conditions (L8 : D16, 400 lux) or under long-day conditions (L16 : D8, 400 lux) for 3 weeks. L12 : D12 conditioned male 3-week-old CBA/N mice (SLC Japan, Shizuoka, Japan) were housed under long-day conditions (L16 : D8, 400 lux) for 3 weeks in Fig. 9A, 10A, and 11B.

For neonatal PT slice culture experiments except Fig. 7A, neonatal wild-type and heterozygous *TSH*β^{Luc} mice were generated by overnight breeding of heterozygous *TSH*β^{Luc} and CBA/N mice. In Fig. 7A, neonatal wild-type and heterozygous *TSH*β^{Luc} mice were generated by *in vitro* fertilization (IVF) of heterozygous *TSH*β^{Luc} and CBA/N mice. Pregnant mice and pups were housed under L12 : D12 conditions (400 lux) because it was reported that exposure to different light/dark conditions from birth affects circadian properties (Ciarleglio *et al.* 2011). For adult PT slice culture experiments, L12 : D12 conditioned 3-week-old wild-type and heterozygous *TSH*β^{Luc} mice were housed under short- or long-day conditions for 2 to 3 weeks. For other experiments, *TSH*β^{Luc} mice were housed under L12 : D12 conditions. All mice were given commercial chow and water *ad libitum* except the supplementation of thyroid powder experiment. Homozygous *TSH*β^{Luc} mice were given commercial chow with 100 ppm thyroid powder (Sigma, St. Louis, MO, USA) and water *ad libitum* (Fig. 1D).

In situ hybridization

Mice were deeply anesthetized with isoflurane (Mylan, Tokyo, Japan) and intracardially perfused with 10 mL saline and 20 mL of a fixative containing 4% paraformaldehyde in 0.1 M phosphate buffer (PB), pH 7.4. Mouse brain samples were post-fixed in the same fixative for 24 h at 4 °C, soaked in PB containing 20% sucrose for several days and stored frozen at −80 °C for further use. *In situ* hybridization was carried

out as previously described (Shigeyoshi *et al.* 1997; Masumoto *et al.* 2010). Serial coronal sections (40 μm thick) of the mouse brain were prepared using a cryostat (CM 1850; Leica Microsystems, Wetzlar, Germany). To prepare probes, fragments of cDNA were obtained by PCR and subcloned into the pGEM-T easy vector (Promega). Radiolabeled probes were generated using ^{35}S-UTP (PerkinElmer, Norwalk, CT, USA) via a standard protocol for cRNA synthesis. The primers used in the construction of *in situ* hybridization cRNA probes were as follows:

TSHβ cRNA probe:

Forward primer: 5′-TGGGTGGAGAAGAGTGAGCG-3′

Reverse primer: 5′-ACCAGATTGCACTGCTATTG-3′

Cga cRNA probe:

Forward primer: 5′-GCAGGCACTGAAAAATCCAGAGACATTGTTC-3′

Reverse primer: 5′-ACACACAGCGCCATTGAATGGCTC-3′

Luc cRNA probe:

Forward primer: 5′-CACCGGTAAGACACTGGGTGTGAACCAGC-3′

Reverse primer: 5′-CACGGCGATCTTGCCGCCCTTCTTGGC-3′

Htr1a cRNA probe:

Forward primer: 5′-TCCCAGCCAAGTCAGCCCCCAAATTCTG-3′

Reverse primer: 5′-CCCTGTCAGTCTCTCAGGTGTGGACACC-3′

Htr1b cRNA probe:

Forward primer: 5′-ATGCTGGACTGCTTTGTGAACACCGACC-3′

Reverse primer: 5′-GGGGTTGATGAGGGAGTTAAGATAGCCTAACC-3′

Htr1d cRNA probe:

Forward primer: 5′-AGCTAGGTCACTGTGTTGTGTAAAGGGGAG-3′

Reverse primer: 5′-AATAGGGTGTCCCATTCAAAGCCTCGAGTG-3′

Htr1f cRNA probe:

Forward primer: 5′-TACAGAGCAGCAAGGACACTGTACCAC-3′

Reverse primer: 5′-ATCCTAATATCGGCATCGTACAAGTTTTTGG-3′

Htr2a cRNA probe:

Forward primer: 5′-AAGCCGCTGCAGTTAATTTTAGTGAACAC-3′

Reverse primer: 5′-GTCACCAACTTACTCCCATGCTACCCATC-3′

Htr2b cRNA probe:

Forward primer: 5′-AGATTTGCTGGTTGGATTGTTTGTGATGC-3′

Reverse primer: 5′-AAAACTGTGGGCACAGTCCACCGTGTTAG-3′

Htr2c cRNA probe:

Forward primer: 5′-TCTTAACTATCAGGGCAAGCTCATAGCAC-3′

Reverse primer: 5′-CTCAGAAGAAGGTAATACACAGGAATAAG-3′

Htr3a cRNA probe:

Forward primer: 5′-TGCTGGCTGTGCTCGCTTACAGCATCACC-3′

Reverse primer: 5′-CCTGCTCCCATTGGCTGATGAAGCTGAG-3′

Htr3b cRNA probe:

Forward primer: 5′-GCAGCAACTGCGTACACTTAGGTTTAAGG-3′

Reverse primer: 5′-ACACCCCCTGCTTTAAATAAGGCAAACTG-3′

Htr4 cRNA probe:

Forward primer: 5′-GTGGACCAATGTATGAATGGCCAGCTGAC-3′

Reverse primer: 5′-CAGTTTAAAAACAAAACCTGTGAAGGTCCCTGTG-3′

Htr5a cRNA probe:

Forward primer: 5′-GACTGTGGACATGTTTCATGTTGATTCCTG-3′

Reverse primer: 5′-CCTAGAGACGGTGTTACATGTGGTTATGC-3′

Htr5b cRNA probe:

Forward primer: 5′-ACGGCCCGATGATGACACTCCAAAAGTC-3′

Reverse primer: 5′-TACGTGTGTCTCCATCAAAAGCAGGCCAC-3′

Htr6 cRNA probe:

Forward primer: 5′-GCCGTATGTGACTGCATCTCTCCAGGTCTC-3′

Reverse primer: 5′-TCTTGACCTGGTCAGTTCATGGGGGAACC-3′

Htr7 cRNA probe:

Forward primer: 5′-CTCTGGAACACCATTCTGTTTCATGTGGAG-3′

Reverse primer: 5′-TACGTTCACTCTAGCGAATCTGCAGCTCAGG-3′

Tshr cRNA probe:

Forward primer: 5′-CAACGATGAAGTAGCCCAGAGGGTCC-3′

Reverse primer: 5′-GGACCGAAGTCATGTAAGGGTTGTCTGTG-3′

Fzd5 cRNA probe:

Forward primer: 5′-GAGAGAGAGAGATTTAGTGACTTTTGATACGGG-3′

Reverse primer: 5′-GACATTTCTTTGTTTTTCATAAATAACTAATCTCC-3′

S1pr3 cRNA probe:

Forward primer: 5′-CACCATCCCCAGCTAGGAGGTGACATTTGTAG-3′

Reverse primer: 5′-CAATCTAACATCATCTACAAGATGGCCCTGGGGG-3′

Cysltr1 cRNA probe:

Forward primer: 5′-TGCTTTGAGCCTCCACAGAACAATCAAGC-3′

Reverse primer: 5′-CGTTACATATTTCTTCTCCTTTTTCTGGCAAGG-3′

Mtnr1a cRNA probe:

Forward primer: 5′-CGGCTCGATATTCAACATCACGGGGATC-3′

Reverse primer: 5′-GCAGCTGTTGAAGTACGCCAGGTAGTAAC-3′

Pkr2 cRNA probe:

Forward primer: 5′-CCTTCAGGTGTTGCCCAAGGAAAAATTTAAC-3′

Reverse primer: 5′-CATTCTTCACAAAGGAAGAGGTGAAAATCACATCC-3′

PT slice culture

*TSH*β^{Luc} mice were decapitated 1–4 h before lights-off (ZT12 for neonatal PT slices, ZT8 or 16 for adult short- or long-day slices). PT slices were prepared from neonatal pups (6–8 days old) or adult mice (5 to 6 weeks old). For neonatal PT slice culture experiments, brains were rapidly removed and were cut by a tissue chopper (McIlwain Tissue Chopper; McIlwain Laboratory Engineering, Gomshall, Surrey, UK) to a thickness of 350 μm. For adult PT slice culture experiments, brains were rapidly removed and were cut by a vibratome type linearslicer (PRO7; Dosaka EM, Kyoto, Japan) to a thickness of 300 μm. The PT region slices were dissected using a surgical knife. The slices were then placed on a culture membrane (MilliCell-CM; Millipore, Bedford, MA, USA) and set on a dish with 1.2 mL culture medium containing DMEM/F12 (Invitrogen, Carlsbad, CA, USA) supplemented with 300 mg/L NaHCO3 (Sigma), 20 mg/L kanamycin (Invitrogen), 100 mg/L apo-transferrin (Sigma), 100 μM putrescine (Sigma), 20 nM progesterone (Sigma), 30 nM sodium selenite (Sigma) and 1 mM luciferin (Biosynth, Staad, Switzerland). In Fig. 7A, B and 11A, 5mg/L insulin (Sigma) was applied to the above medium because experimental condition was not fixed in these stages. The dish was sealed with silicone grease (HVG; Dow Corning-Toray, Tokyo, Japan). Explants from different pups were cultured separately, and only those of appropriate genotypes were chosen for further experiments. Slices were treated with reagents as specified in each experiment. Reagents were obtained from the following sources: forskolin, gulutamine, glutamic acid, 6-Bnz-cAMP (PKA agonist), MDL-12,330A (MDL), pertussis toxin (PTX), m-3M3FBS, 12-*O*-tetradecanoyl phorbol 13-acetate (TPA), KCl, serotonin, alpha-amino-3-hydroxy-5-methyl-4-isoxazolepropionic acid (AMPA), N-methyl-D-aspartic acid (NMDA), kainic acid (KA), and TSH from bovine pituitary from Sigma; 8-pCPT-2′-*O*-Me-cAMP (Epac agonist) from Biolog (Bremen, Germany); recombinant prokineticin 2 was kindly provided by Dr. Zhou. Reagents were solubilized in water, ethanol or dimethylsulfoxide (DMSO) to make stock solutions

40-1000x the working solutions. Serotonin was solubilized in 0.1 N HCl. Kainic acid was solubilized in 1N NaOH and adjusted to the appropriate volume by the addition of water. Glutamine, glutamic acid, serotonin, AMPA, NMDA, and KA aliquots were made fresh each day. For glutamine and glutamic acid starvation, culture medium with DMEM/F12 without glutamine and glutamic acid (Cell Science & Technology Institute, Sendai, Japan) was used. For glutamine, glutamic acid, AMPA, NMDA, or KA treatments, the glutamine- and glutamic acid–starved culture medium was replaced with the above fresh culture medium or with added vehicle, glutamine, glutamic acid, AMPA, NMDA, or KA (Fig. 5, 12). For ionomycin treatment, PT slices on culture membranes were transferred to other dishes containing fresh medium with ionomycin for 30 min. PT slices on culture membranes were returned to the previous dishes and the dishes were then immediately returned to the PMT and monitoring was restarted (Fig. 7C). For melatonin removal and forskolin treatment, PT slices on culture membranes were transferred to other dishes containing fresh medium with vehicle or forskolin. The dishes were then immediately returned to the PMT and monitoring was restarted (Fig. 8). In Fig. 9C, serotonin was applied at approximately 12 h after the start of the culture to neonatal PT slices from CD-1 mice.

Quantitative RT-PCR (qPCR)

For qPCR experiments of the pituitary composed of the anterior and posterior lobes, *TSH*β^{Luc} mice were decapitated at ZT2 to 6 under L12 : D12 conditions to collect the part of the tissue embedded in the sella turcica (pituitary fossa) from 12-week-old male *TSH*β^{Luc} mice and temporarily stocked at −80 °C for further use. The total RNA was prepared from each pituitary, using RNeasy micro kit (Qiagen, Valencia, CA, USA). The cDNAs were synthesized from 0.25 μg of the total RNA using Superscript III transcriptase (Invitrogen). qPCR was performed using SYBR Green PCR Master Mix (Applied Biosystems, Foster City, CA, USA).

For qPCR experiments of the cultured PT samples, the cultured PT samples were collected 48 h after the start of the culture. The total RNA was prepared from each cultured PT, using NucleoSpin RNA XS kit (Takara, Otsu, Japan). The cDNAs were synthesized from 0.05 μg of the total RNA of the cultured PT using Superscript Vilo transcriptase (Invitrogen).

qPCR was performed using Quantitect SYBR Green PCR mastermix (Qiagen). qPCR was performed using the ABI PRISM 7900 (Applied Biosystems) at the following conditions: Samples contained 1 × SYBR Green PCR Master Mix or QuantiTect SYBR Green PCR Master Mix, 0.8 μM primers and 1/50 synthesized cDNA in a 10-μL volume. The PCR conditions were as follows: 10 min at 95 °C, then 45 cycles of 15 s at 94 °C, 1 min at 59 °C. The absolute cDNA abundance was calculated using a standard curve obtained from murine genomic DNAs. I used *TATA box-binding protein* (*Tbp*) or *actin, beta* (*Actb*)

as the internal controls. Primer information is as follows:

*TSH*β mRNA (exon 4):

Forward primer: 5′-GTGGGCAAGCAGCATCCTTTTG-3′

Reverse primer: 5′-GCACACTCTCTCCTATCCACGTAC-3′

Cga mRNA:

Forward primer: 5′-TGCTGAGCCGAGCCATTCAATG-3′

Reverse primer: 5′-GAAGTCTGGTAGGGAGGAGGTGG-3′

Luc mRNA:

Forward primer: 5′-TCCTCAACGTGCAAAAGAAGCTACC-3′

Reverse primer: 5′-GTCGGTCTTGCTATCCATGATGATGATC-3′

Actb mRNA:

Forward primer: 5′-TTGTCCCCCCAACTTGATGT-3′

Reverse primer: 5′-CCTGGCTGCCTCAACACCT-3′

*TSH*β mRNA:

Forward primer: 5′-CTGCATACACGAGGCTGTCAG-3′

Reverse primer: 5′-CCCCAGATAGAAAGACTGCGG-3′

Eya3 mRNA:

Forward primer: 5′-TTCACAGCTCCAAGTAGAATCTGACT-3′

Reverse primer: 5′-TATGGAAGCGCCATGAGCTT-3′

Tbp mRNA:

Forward primer: 5′-CCCCCTCTGCACTGAAATCA-3′

Reverse primer: 5′-GTAGCAGCACAGAGCAAGCAA-3′

PMT bioluminescence measurements

The time-course bioluminescence results were obtained as reported previously (Isojima *et al.* 2009). PMT measurements with a high-sensitivity bioluminescence detection system (LM-2400; Hamamatsu Photonics, Hamamatsu, Japan) were started immediately after the start of PT slice culture at the time of lights-off (ZT12 for neonatal PT slices, ZT8 or 16 for adult short- or long-day slices). For the data analysis in Fig. 3B and D, raw photon counts were plotted. For the data analysis in Figs 3C, E, 5-8, 9B, 10B, 11A and 12, photon counts of the PT slice from heterozygous *TSH*β^{Luc} mice were calculated by subtracting background photon counts of PT slice from wild-type mice. For experiments in which reagents were added at the start of the culture, the resultant values were further normalized by photon counts at ZT4.75, which is 12.75 h after the start of the culture in adult long-day slices (Fig. 3C), or at

ZT23, which is 11 h after the start of the culture in neonatal PT slices (Fig. 3E, 6D, E, 7D, and 10B), which were the median time for the lowest bioluminescence values from all vehicle-treated samples in adult and neonatal slices, respectively (Fig. 13). For experiments in which reagents were added after the start of the culture, the resultant values were normalized by photon counts at ZT13.45, ZT19.75, ZT3.75, or ZT11.75 which are just before reagent treatments in neonatal PT slices (Fig. 5, 6B, C, 6F, 7A-C, 8, 9B, 11A, and 12). In Fig. 6A, the resultant values were further normalized by photon counts at ZT22.75, which is 10.75 h after the start of the culture in vehicle-treated samples, or at ZT11, which is 23 h after the start of the culture in forskolin-treated samples, which were the lowest bioluminescence values from each sample.

Bioluminescence imaging

Samples were prepared as described above. Sealed 35-mm culture dishes were placed on the stage of a macrozoom microscope (MVX10; Olympus, Tokyo, Japan) in a dark hood. The culture dishes were kept at approximately 37 °C in a heated chamber (Tokai Hit, Shizuoka, Japan) on the microscope stage. Bioluminescence was imaged using a 1.6 × Plan Apochromat objective (NA 0.24; Olympus) with 6.3 × zoom and transmitted to an electron-multiplying charge-coupled device (EM-CCD) camera cooled to −80 °C (ImagEM; Hamamatsu Photonics). The dimension of an image is 512 × 512 pixels, and each pixel corresponds to the size of 1.587 × 1.587 μm. Exposure time was 29 min with EM gain of 200 × for snapshot images, and exposure time was 14 min with EM gain of 300 × for time-lapse images. Images were transferred at 690 KHz to minimize readout noise, and analyzed using MetaMorph software (Molecular device, Sunnyvale, CA, USA). Single-cell tracking was performed as previously described (Ukai *et al.* 2007).

Fluoxetin and paroxetin administration

Male 3-week-old CBA/N mice were singly housed under L12 : D12 conditions (400 lux) with food and water available *ad libitum*. 5-week-old mice were acclimated to 0.2% saccharin water for 1 week. Fluoxetin and paroxetin administration was carried out as previously described (Kobayashi *et al.* 2008; Kobayashi *et al.* 2010; Kobayashi *et al.* 2011). Fluoxetine hydrochloride (Wako Pure Chemical Industries, Ltd., Osaka, Japan) and paroxetine hydrochloride (Toronto Research Chemicals Inc., Toronto, Canada) were orally applied to 6-week-old mice for 2 weeks at a dose of 10 or 22 mg/kg/ day and 10 or 30 mg/kg/ day, respectively. The fluoxetine solutions and the paroxetin solutions were prepared everyday, and concentrations of fluoxetine and paroxetin were determined for individual mice based on the water consumption during preceding 24 h and the body weight measured every other day. 0.2% saccharin was

included in the fluoxetine solution and the paroxetin solution. Control mice were given water with or without saccharin, and all data were pooled. After 2 weeks of fluoxetine and paroxetine administration, mouse brain samples were collected to perform RI *in situ* hybridization.

Mass spectrometry

The YALSQDVCTYR peptide, which was the unique sequence for TSHβ, was synthesized on a peptide synthesizer (Syro Wave; Biotage, Uppsala, Sweden) using Fmoc solidphase chemistry. The peptide was dimethyl-labeled with formaldehyde (CD_2O) and desalted by C18 StageTips according to previously described method (Boersema *et al.* 2009). The dimethyl labeling of the peptide was checked by liquid chromatography coupled with tandem mass spectrometry (LC-MS/ MS) with an LTQ orbitrap velos mass spectrometer (Thermo scientific, Waltham, MA, USA) coupled to a nano-Advance UHPLC system (Bruker Daltonics, Leipzig, Germany).

The culture medium of the PT slices was collected and temporarily stocked at −80 °C for further use. Proteolytic digestion was performed using a phase-transfer surfactant protocol (Masuda *et al.* 2008; Narumi *et al.* 2012). The resultant digest was dimethyl-labeled with formaldehyde (CH_2O).

For quantification by mass spectrometry, a triple quadrupole mass spectrometer (TSQ Vantage EMR; Thermo scientific) was used to design a selected reaction monitoring (SRM) method. LC-SRM/MS was performed by a TSQ Vantage EMR mass spectrometer equipped with a nanoLC interface (AMR), a nano-Advance UHPLC system (Bruker Daltonics) and an HTC-PAL autosampler (CTC Analytics, Basingstoke, UK). The parameters of the mass spectrometer were set as follows: 0.002 m/z scan width, 40 msec scan time, 0.7 fwhm Q1 and Q3 resolution and 1.8 mTorr gas pressure.

For data analysis of the peak area in the chromatogram of each SRM transition, the peak area was extracted by using Pinpoint software (Thermo scientific). To confirm whether the peaks of SRM chromatogram were derived from the endogenous YALSQDVCTYR peptide, we checked that ratios among the peak areas of 6 SRM transitions were comparable with those of the standard YALSQDVCTYR peptide. Three of six SRM transitions, which had a lower variability in the ratio between the 18 runs of LC-SRM/MS analysis, were used for the quantification of the endogenous YALSQDVCTYR peptide. Chromatograms of SRM transition are shown in Fig. 14. Interassay coefficient of variation was 7.9%. The lower limit of sensitivity was 13.27 attomole.

Statistical analyses

All data are shown as means ± SEM. Comparison of two groups was made using two-sample *t*-test. A value of $P < 0.05$ was considered as statistically significant. The analyses were performed by Microsoft

Excel (Microsoft, Redmond, WA, USA) or R software (see The Foundation for Statistical Computing, http://www.R-project.org).

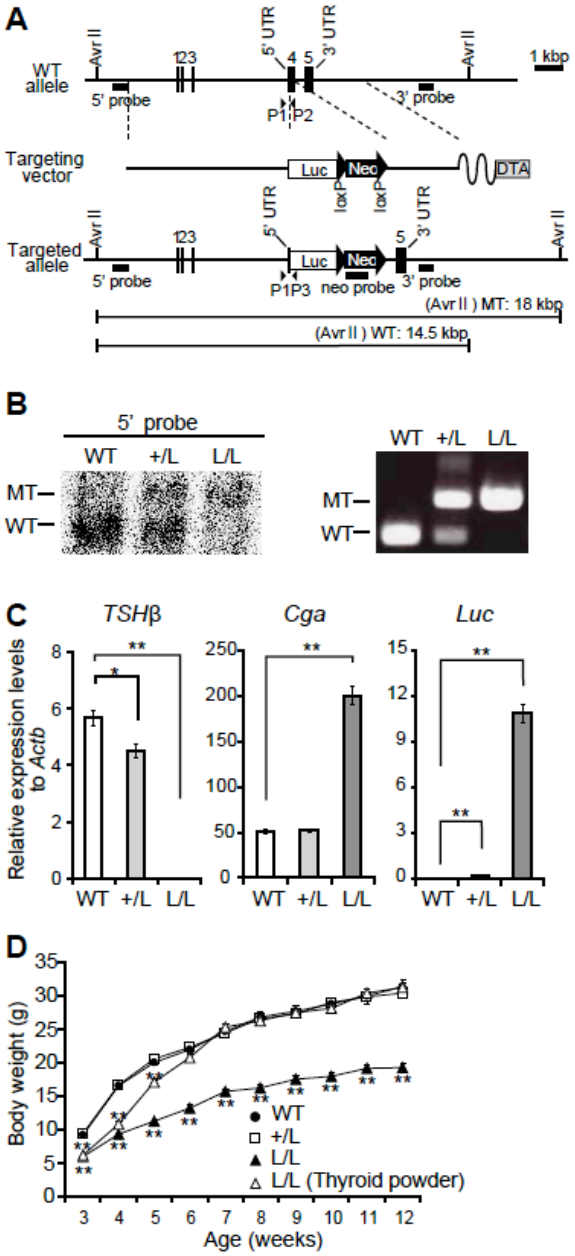

Figure 1. Generation of *TSH*β^{Luc} mice. (A) Targeting schema. Exons 1–5 are indicated by solid boxes. *TSH*β ORF is indicated by filled boxes. *Luc* ORF sequence was inserted in frame to the first ATG of exon 4 of the *TSH*β gene. The hybridization probes used for Southern blot analysis (5′, 3′ and Neo probes) and PCR primers for routine genotyping (P1-P3) are indicated by bold black lines and black arrowheads, respectively. (B) Southern blot analysis of the 5′ region (left) and genotyping PCR (right). Wild-type allele, heterozygous and homozygous mutant alleles are indicated as WT, +/L and L/L, respectively. One extra band was appeared in the +/L lane in genotyping PCR (right). (C) Expression levels of *TSH*β, *Cga* and *Luc* in the pituitary of *TSH*β^{Luc} mice by using quantitative RT-PCR (qPCR). The statistical

differences between wild-type and heterozygous or homozygous *TSH*β^{Luc} mice were calculated. *P < 0.05; **P < 0.01 (two-sample t-test, n = 6–8, average ± SEM). (D) Growth curves in male *TSH*β^{Luc} mice. The statistical differences between wild-type and heterozygous or homozygous *TSH*β^{Luc} mice were calculated. **P < 0.01 (two-sample t-test, n = 6–8, average ± SEM).

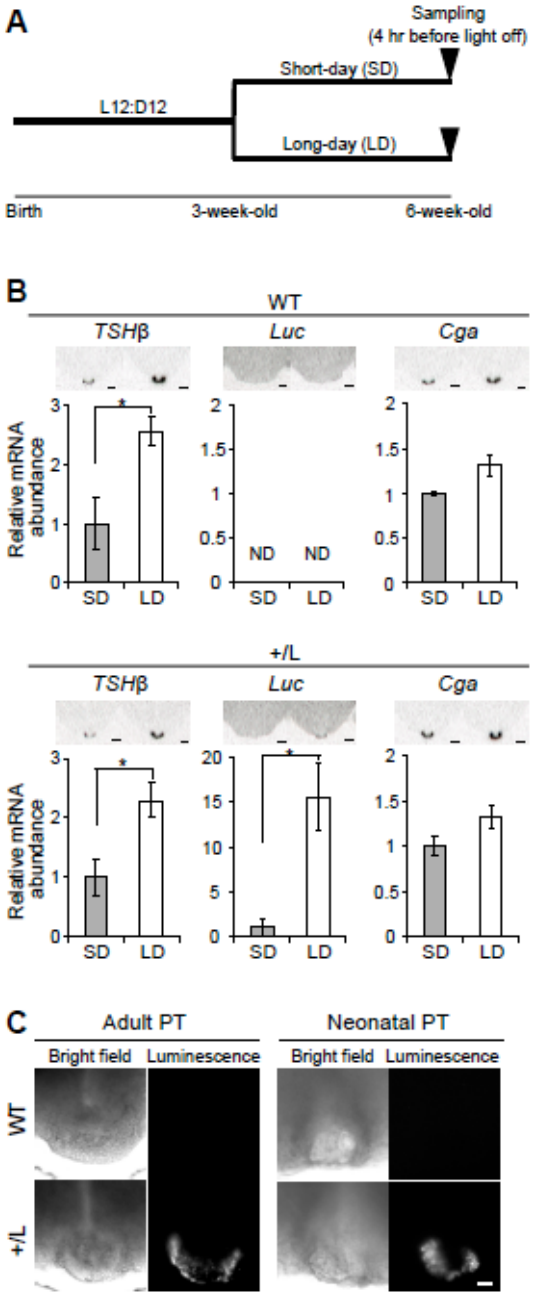

Figure 2. Photoperiodic gene responses in *TSH*β^{Luc} mice. (A) Experimental schema. 3-week-old mice were transferred to short-day (SD; light/dark = 8:16 hour) or long-day (LD; light/dark = 16:8 h) conditions and maintained for 3 weeks. Brain samples were collected 4 h before lights-off (ZT4 of SD and ZT12 of LD). (B) Expressions of *TSH*β, *Luc* and *Cga* under SD and LD conditions in wild-type (WT) and heterozygous *TSH*β^{Luc} mice (+/L) measured by radioisotope (RI) *in situ* hybridization. The signal intensities were quantified and normalized by the values in SD samples except *Luc* measurement in WT mice. Scale bar: 300 μm. ND, not detected. *$P < 0.05$ (two-sample *t*-test, n = 3–5, average ± SEM). (C)

Bioluminescence imaging of the PT. Adult PT slices were prepared from LD conditioned mice and neonatal PT slices were prepared from L12 : D12 conditioned mice. Bright-field and corresponding bioluminescence CCD images captured from the representative PT slices are shown. Scale bar: 100 μm (see also Fig. 4).

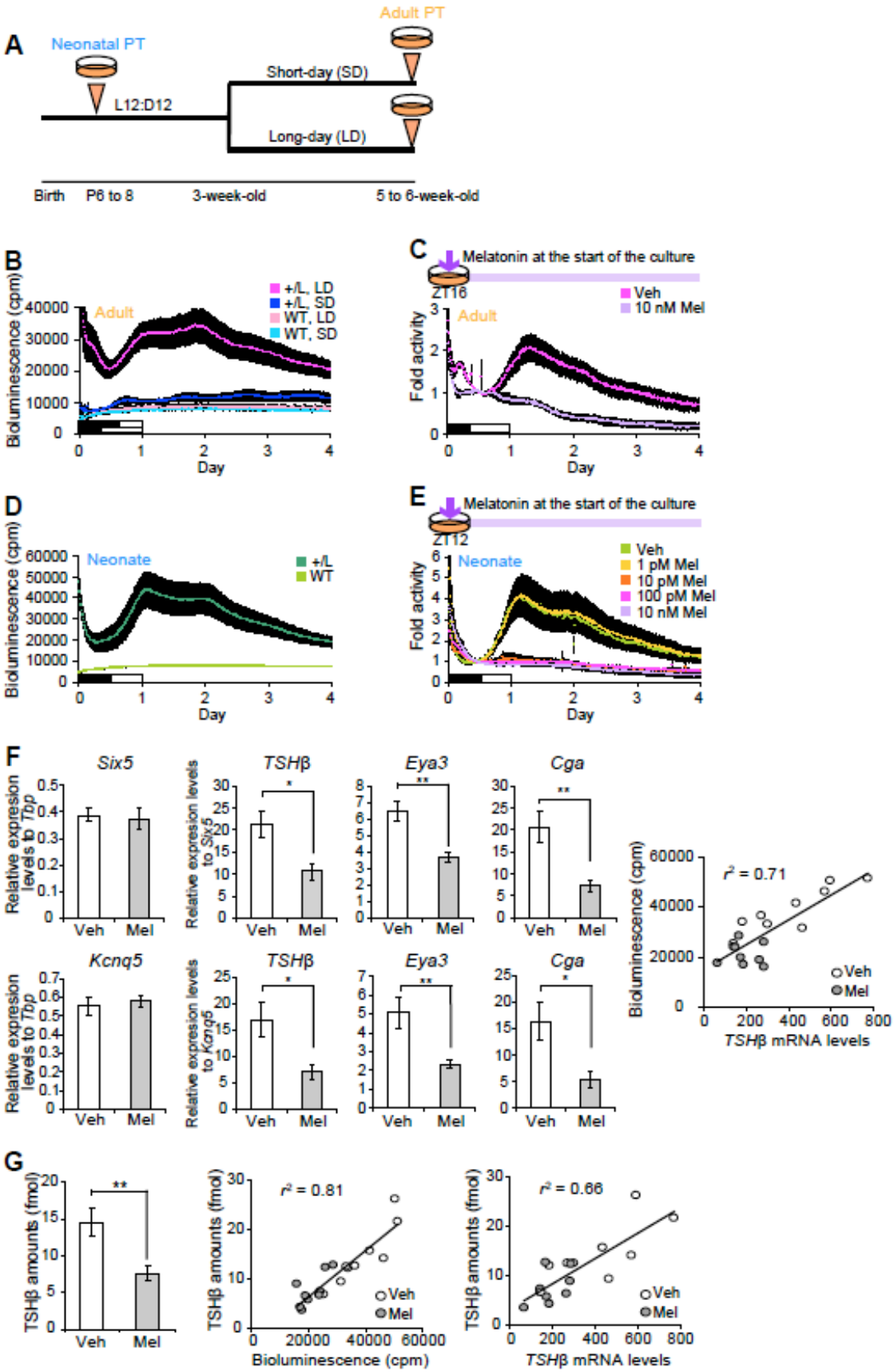
A
Neonatal PT
Adult PT
L12:D12
Short-day (SD)
Long-day (LD)
Birth
P6 to 8
3-week-old
5 to 6-week-old
B
Bioluminescence (cpm)
Adult
+/L, LD
+/L, SD
WT, LD
WT, SD
Day
C
Melatonin at the start of the culture
ZT16
Veh
10 nM Mel
Fold activity
Adult
Day
D
Bioluminescence (cpm)
Neonate
+/L
WT
Day
E
Melatonin at the start of the culture
ZT12
Veh
1 pM Mel
10 pM Mel
100 pM Mel
10 nM Mel
Fold activity
Neonate
Day
F
Six5
TSHβ
Eya3
Cga
Relative expression levels to Tbp
Relative expression levels to Six5
Veh
Mel
Kcnq5
Relative expression levels to Kcnq5
Bioluminescence (cpm)
r² = 0.71
TSHβ mRNA levels
G
TSHβ amounts (fmol)
r² = 0.81
Bioluminescence (cpm)
r² = 0.66
TSHβ mRNA levels

Figure 3. Real-time monitoring of the *TSH*β expression by bioluminescence. (A) Experimental schema. Neonatal PTs were collected at postnatal 6–8 (P6–8) under L12 : D12 conditions, and 5- to 6-week-old mice were collected after being maintained in short-day (SD) or long-day (LD) conditions for 2–3 weeks. (B and D) Real-time bioluminescence recording in adult or neonatal PT slices of indicated genotypes. White and black bars on the graphs indicate the subjective day and night on the following days after sampling, respectively [n = 2, wild-type (WT) mice or n = 6, heterozygous *TSH*β^{Luc} mice (+/L) in B; n = 5, WT and n = 17, +/L in D, average ± SEM]. (C and E) Real-time monitoring of the luciferase (luc) reporter activities in adult or neonatal PT slices after the addition of vehicle (Veh) or melatonin (Mel). The PT slices were prepared from animals kept under LD (adult, C) or L12 : D12 (neonate, E) conditions. Vehicle or melatonin was applied at the start of the culture. Data were normalized by the values of photon count at ZT4.75 (adult, C) or ZT23 (neonate, E, see Experimental procedures). Normalized luc reporter activities of PT slices from +/L mice are shown (n = 4 in C and n = 3–4 in E, average ± SEM). (F) Confirmation of expression level changes in *TSH*β, *Eya3* and *Cga* in the cultured PT by qPCR analysis. Neonatal PT slices were treated with vehicle or 10 nM melatonin 48 h with PMT monitoring. Expression levels of *TSH*β, *Eya3* and *Cga* were normalized by the value of *Six5* or *Kcnq5*, which were specifically expressed in the PT. **P* < 0.05; ***P* < 0.01 (two-sample *t*-test, n = 9, average ± SEM). Correlation between *TSH*β mRNA levels and bioluminescence counts (right). White circles (Veh) and gray circles (Mel) indicate data points. The line is regression: r^2 = 0.71. (G) Quantification of secreted amounts of *TSH*β into the culture medium of the PT slices in 3F by mass spectrometry analysis. ***P* < 0.01 (two-sample *t*-test, n = 9, average ± SEM). Correlation between secreted *TSH*β amounts (middle) and *TSH*β mRNA levels or bioluminescence counts (right). White circles (Veh) and gray circles (Mel) indicate data points. The line is regression: r^2 = 0.81 (middle), r^2 = 0.66 (right).

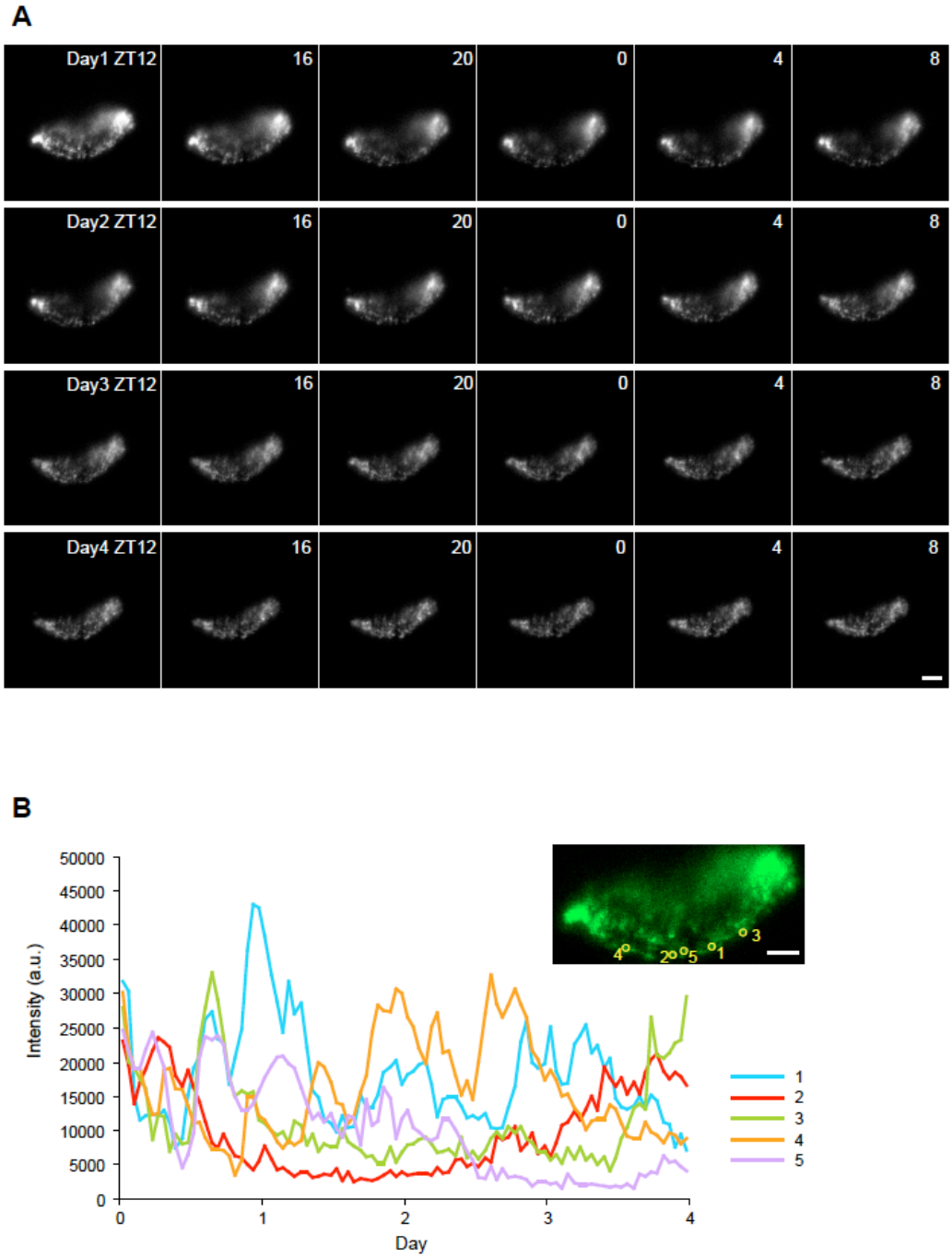

Figure 4. Time-lapse bioluminescence imaging of the PT. (A) Time-lapse images of neonatal PT slice from heterozygous *TSH*β^{Luc} mice kept under L12:D12 conditions. Scale bar: 100 μm. (B) Representative bioluminescence patterns in individual neonatal PT cells in Fig. 4A. Scale bar: 100 μm.

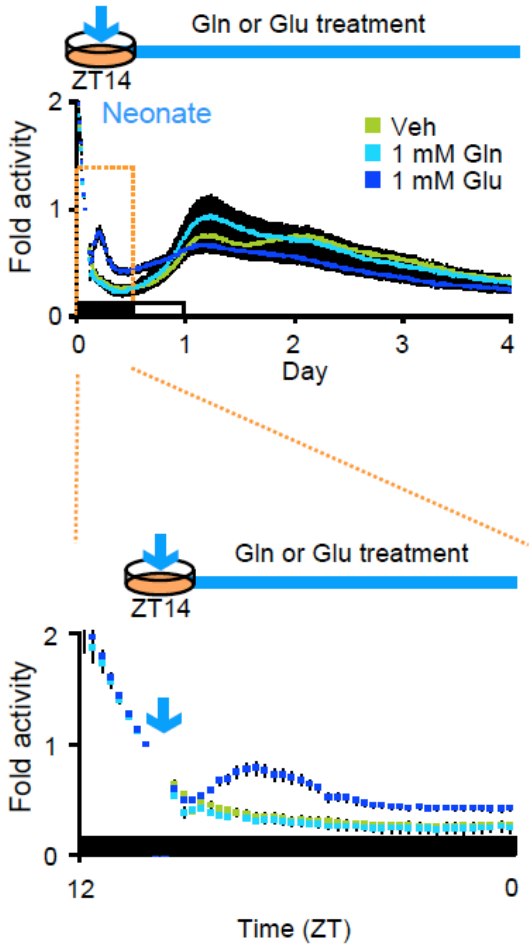

Figure 5. Real-time monitoring of the luciferase reporter activities in neonatal PT slices with glutamine or glutamic acid treatment. 1 mM glutamine (Gln) or 1 mM glutamic acid (Glu) containing medium and control medium that does not contain glutamine and glutamic acid (Veh) was replaced 2 h after glutamine and glutamic acid starvation from the start of the culture. Lower panel shows data that are 12 h after the start of the culture in upper panel. Normalized luciferase reporter activities of neonatal PT slices from heterozygous *TSHβ*^{Luc} mice kept under L12:D12 conditions are shown. (n = 5, average ± SEM). White and black bars on the graphs indicate the subjective day and night on the following days after sampling, respectively. ZT12 is the start of subjective night and the culture was started at the time point.

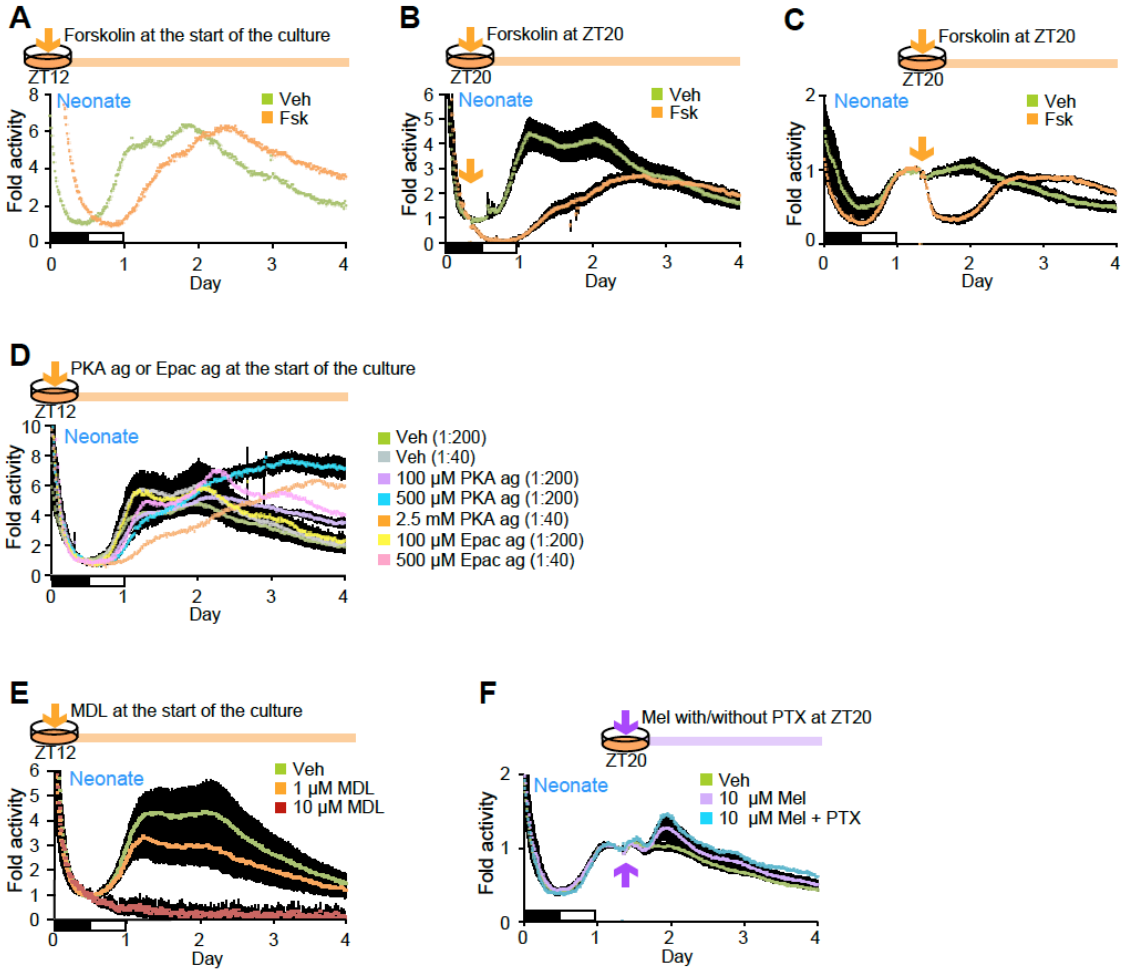

Figure 6. Effects of drugs targeting the cAMP signal on bioluminescence activity. Real-time monitoring of the luciferase (luc) reporter activities in the neonatal PT slices with vehicle (Veh) or reagents. (A-C) An adenylate cyclase activator (Fsk, forskolin) treatment. (A) Vehicle or 1 μM of forskolin was applied at the start of the culture. Data were normalized by the lowest values of photon count in each condition. (B) Vehicle or 1 μM of forskolin was applied at 8 h after the start of the culture. Data were normalized by the values of photon count just before treatment. (C) Vehicle or 1 μM of forskolin was applied at 8+24 h after the start of the culture. Data were normalized as in (B). Normalized luc reporter activities of neonatal PT slices from heterozygous *TSHβ*^{Luc} mice housed under L12:D12 conditions are shown (n = 1 in A, n = 3-5 in B, and n = 3-4 in C, average ± SEM). (D) A protein kinase A (PKA) agonist (PKA ag, 6-Bnz-cAMP) or an exchange protein directly activated by cAMP (Epac) agonist (Epac ag, 8-CPT-2′-*O*-Me-cAMP) treatment. Vehicle, PKA ag or Epac ag was applied at the start of the culture. Vehicle (dilution 1 : 200 or 1 : 40), 100 or 500 μM of PKA ag (dilution 1:200), 2.5 mM of PKA ag (dilution 1:40), 100 μM Epac ag (dilution 1:200), or 500 μM of Epac ag (dilution 1:40) was applied to medium. Data were normalized by

the values of photon count at ZT23. Normalized luc reporter activities of neonatal PT slices from heterozygous *TSH*β^{Luc} mice housed under L12:D12 conditions are shown (n = 1-3, average ± SEM). (E) An adenylate cyclate inhibitor (MDL, MDL-12,330A) treatment. Vehicle, 1 or 10 μM of MDL was applied at the start of the culture. Data were normalized by the values of photon count at ZT23. Normalized luc reporter activities of neonatal PT slices from heterozygous *TSH*β^{Luc} mice housed under L12:D12 conditions are shown (n = 3, average ± SEM). (F) Melatonin (Mel) and pertussis toxin (PTX) treatment. Vehicle, 10 μM of melatonin with/without 1 μg / mL of PTX was applied at 8+24 h after the start of the culture. Data were normalized by the values of photon count just before treatment. Normalized luc reporter activities of neonatal PT slices from heterozygous *TSH*β^{Luc} mice housed under L12:D12 conditions are shown (n = 1-3, average ± SEM). White and black bars on the graphs indicate the subjective day and night on the following days after sampling, respectively. ZT12 is the start of subjective night and the culture was started at the time point.

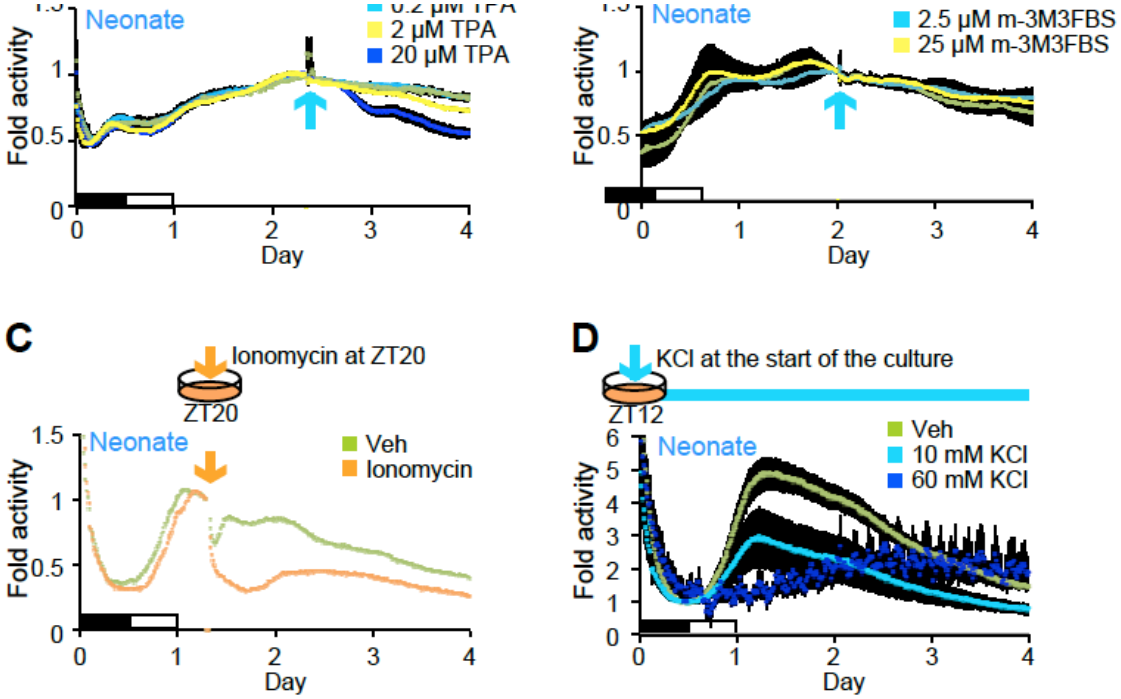

Figure 7. Effects of drugs targeting intracellular signaling pathways on bioluminescence activity. Real-time monitoring of the luciferase (luc) reporter activities in the neonatal PT slices with vehicle (Veh) or reagents. (A) A protein kinase C activator (TPA, 12-*O*-tetradecanoyl phorbol 13-acetate) treatment. Vehicle, 0.2, 2, or 20 μM of TPA was applied at 8+48 h after the start of the culture. (B) A phospholipase C activator (m-3M3FBS) treatment. Vehicle, 2.5 or 25 μM of m-3M3FBS was applied at 8+48 h after the start of the culture. (C) A calcium ionophore (ionomycin) treatment. Vehicle or 1 μM of ionomycin was applied for 30 min at 8+24 h after the start of the culture. (D) KCl treatment. Vehicle, 10 or 60 mM of KCl was applied at the start of the culture. Data were normalized by the values of photon count just before treatment (A-C) or at ZT23. Normalized luc reporter activities of neonatal PT slices from heterozygous *TSH*β^{Luc} mice housed under L12:D12 conditions are shown (n = 2-4 in A, n = 3-5 in B, n = 1 in C, and n = 3 in D, average ± SEM). White and black bars on the graphs indicate the subjective day and night on the following days after sampling, respectively. ZT12 is the start of subjective night and the culture was started at the time point. The measurement was started at ZT12 (A, C and D) or ZT20 (B).

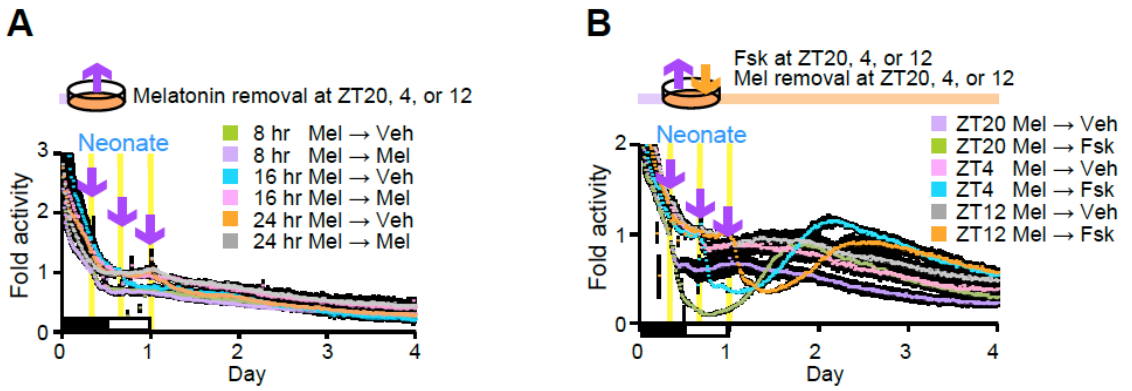

Figure 8. Time-dependency of bioluminescence activity to melatonin removal with/without forskolin treatment. Real-time monitoring of the luciferase (luc) reporter activities in the neonatal PT slices with treatments at different three timings. (A) Melatonin removal. 10 pM of melatonin (Mel) was applied at the start of the culture. Culture medium was replaced with the fresh culture medium with vehicle (Veh) or 10 pM of melatonin at ZT20, 4, or 12, which are 8, 16, or 24 h after the start of the culture, respectively. (B) Melatonin removal with vehicle or forskolin (Fsk) treatment.10 pM of melatonin was applied at the start of the culture. Melatonin was removed and vehicle or 1 μM of forskolin was applied by medium changing at ZT20, 4, or 12, which are 8, 16, or 24 h after the start of the culture, respectively. Data were normalized by the values of photon count just before treatment. Normalized luc reporter activities of neonatal PT slices from heterozygous *TSH*β^{Luc} mice housed under L12:D12 conditions are shown (n = 3 in A and n = 3 in B, average ± SEM). White and black bars on the graphs indicate the subjective day and night on the following days after sampling, respectively. ZT12 is the start of subjective night and the culture was started at the time point.

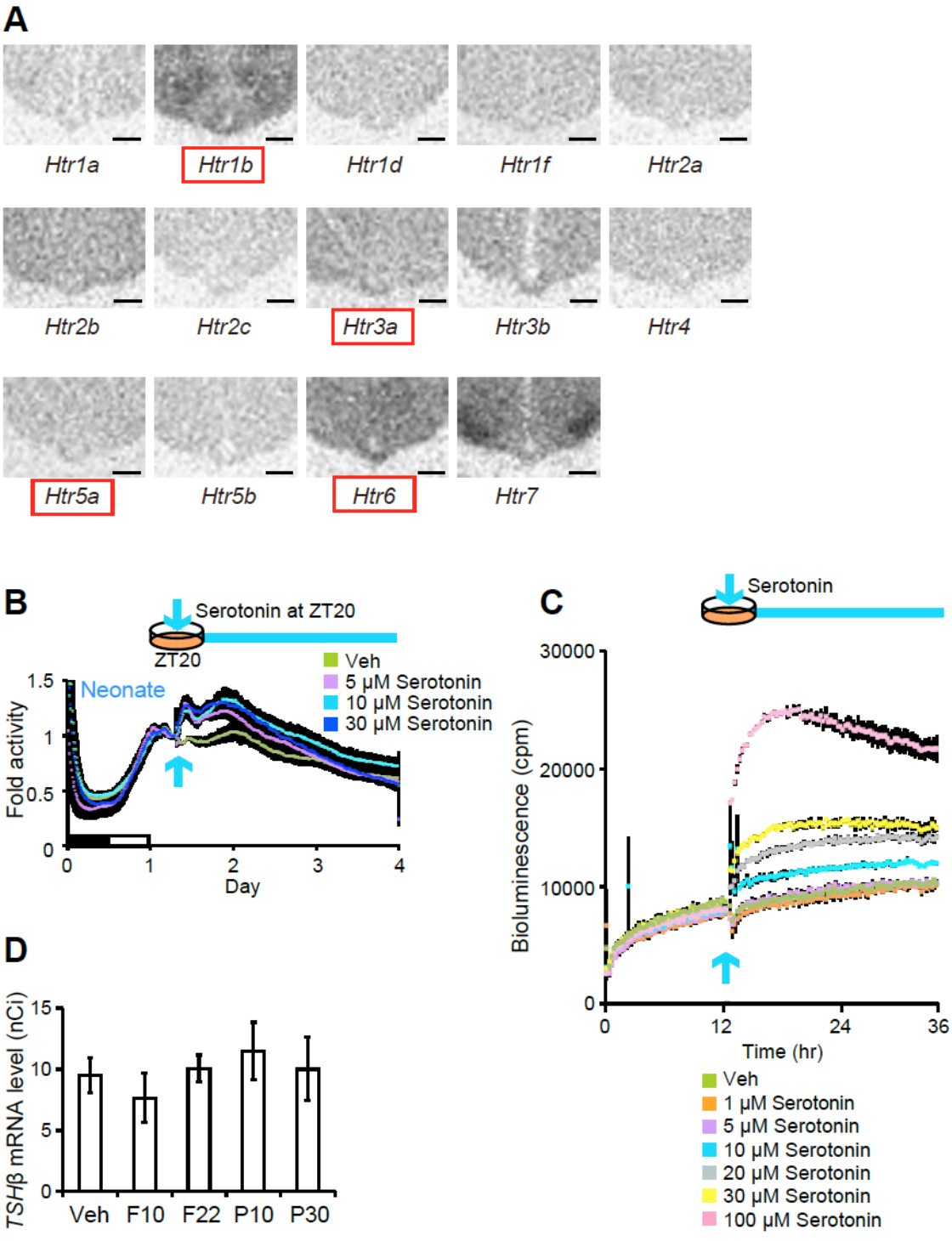

Figure 9. Serotonin effects on *TSH*β expression. (A) Expression patterns of serotonin receptor subtypes. Expression patterns of serotonin receptor subtypes in CBA/N mice were analyzed by radioisotope (RI) *in situ* hybridization. Red boxes indicate the serotonin receptor subtypes expressed in the PT. Scale bar: 300 μm. (B) Real-time monitoring of the luciferase (luc) reporter activities in the neonatal PT slices with

vehicle (Veh) or serotonin treatment. Vehicle, 5, 10, or 30 μM of serotonin was applied at 8+24 h after the start of the culture. Data were normalized by the values of photon count just before treatment. Normalized luc reporter activities of neonatal PT slices from heterozygous *TSH*β^{Luc} mice housed under L12:D12 conditions are shown (n = 3-4, average ± SEM). White and black bars on the graphs indicate the subjective day and night on the following days after sampling, respectively. ZT12 is the start of subjective night and the culture was started at the time point. (C) Intrinsic fluorescence of serotonin was measured by PMT. Raw photon counts are shown (n = 2-3, average ± SEM). Vehicle or serotonin was applied at approximately 12 h after the start of the culture to the neonatal PT slices from CD-1 mice that do not carry the luciferase reporter. (D) Selective serotonin reuptake inhibitors (SSRIs) administration. Vehicle, 10 or 22 mg/kg/day of fluoxetine (F10 or F22), or 10 or 30 mg/kg/day of paroxetine (P10 or P30) was chronically administrated for 2 weeks to short-day conditioned CBA/N mice. Expression of *TSH*β was measured by radioisotope (RI) *in situ* hybridization. There was no significant difference between vehicle- and SSRIs-administrated groups (two-sample *t*-test, n = 3, average ± SEM).

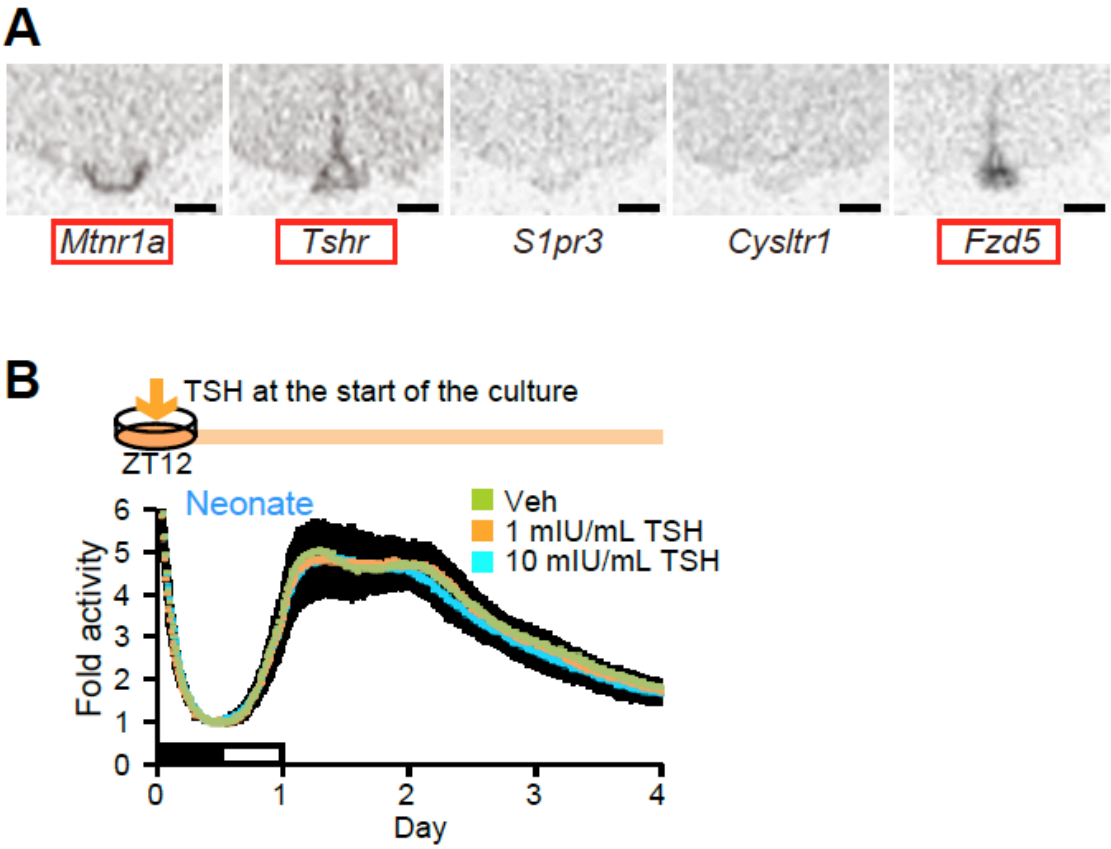

Figure 10. Screening of candidate G-protein coupled receptors (GPCRs). (A) Expression patterns of candidate GPCRs. Expressions of melatonin receptror (*Mtnr1a*), TSH receptor (*Tshr*), *S1pr3*, *Cysltr1*, and *Fzd5* in CBA/N mice were measured by radioisotope (RI) *in situ* hybridization. Red boxes indicate the candidate GPCRs expressed in the PT. Scale bar: 300 μm. (B) Real-time monitoring of the luciferase (luc) reporter activities in the neonatal PT slices with vehicle (Veh) or thyroid stimulating hormone (TSH) treatment. Vehicle, 1 or 10 mIU/mL of TSH was applied at the start of the culture. Data were normalized by the values of photon count at ZT23. Normalized luc reporter activities of neonatal PT slices from heterozygous *TSH*β^{Luc} mice housed under L12:D12 conditions are shown (n = 2-3, average ± SEM). White and black bars on the graphs indicate the subjective day and night on the following days after sampling, respectively. ZT12 is the start of subjective night and the culture was started at the time point.

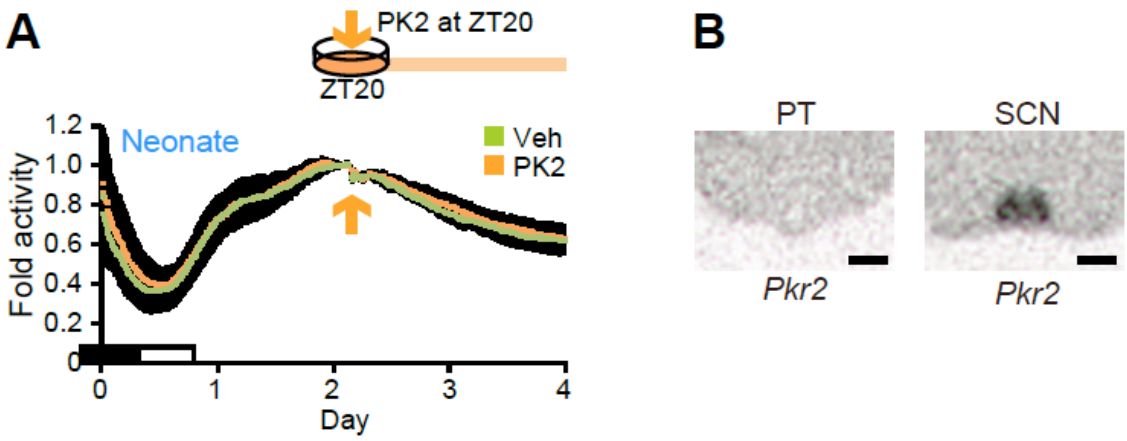

Figure 11. Prokineticin 2 (PK2) effects on bioluminescence activity. (A) Real-time monitoring of the luciferase (luc) reporter activities in the neonatal PT slices with vehicle (Veh) or recombinant PK2 treatment. Vehicle or 20 nM of recombinant PK2 was applied at 8+48 h after the start of the culture. Data were normalized by the values of photon count just before treatment. Normalized luc reporter activities of neonatal PT slices from heterozygous *TSH*β^{Luc} mice housed under L12:D12 conditions are shown (n = 5-6, average ± SEM). White and black bars on the graphs indicate the subjective day and night on the following days after sampling, respectively. ZT12 is the start of subjective night and the culture was started at the time point. The measurement was started at ZT17. (B) Expression patterns of *prokineticin receptor 2* (*Pkr2*). Expression pattern of *Pkr2* in CBA/N mice was analyzed by radioisotope (RI) *in situ* hybridization. *Pkr2* was not detected in the PT (left). Signal was detected in the SCN, which is a positive control tissue (right) (Cheng *et al.* 2002). Scale bar: 300 μm.

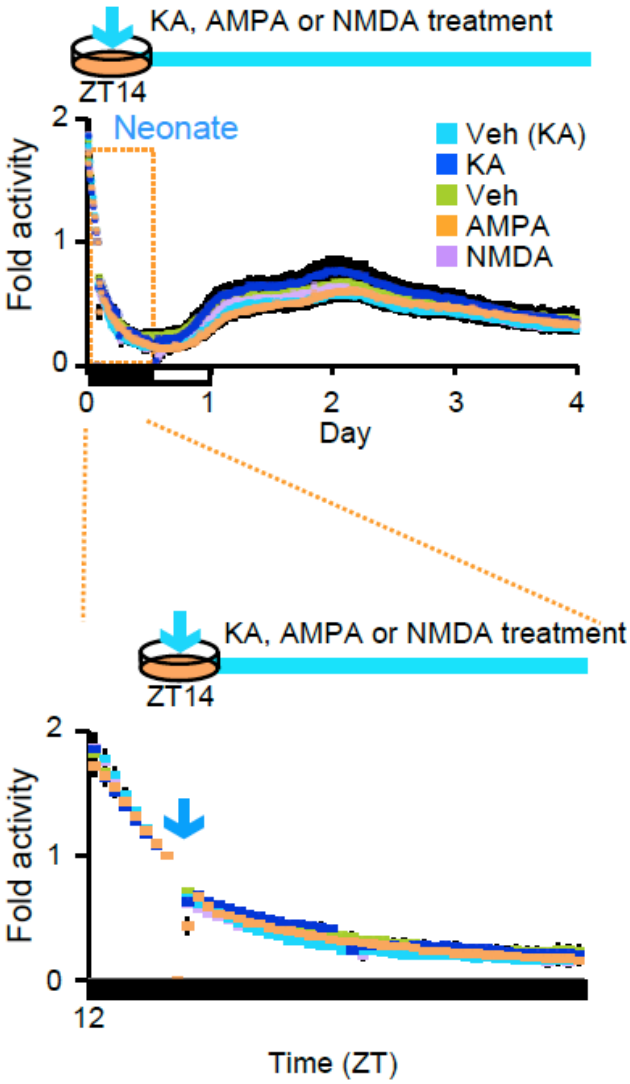

Figure 12. Effects of glutamic acid receptor agonists on bioluminescence activity. Real-time monitoring of the luciferase (luc) reporter activities in the neonatal PT slices with vehicle (Veh), kainic acid (KA), alpha-amino-3-hydroxy-5-methyl-4-isoxazolepropionic acid (AMPA), or N-methyl-D-aspartic acid (NMDA) treatment. 50 μM of KA, 50 μM of AMPA, or 50 μM of NMDA containing medium or control medium that does not contain glutamine and glutamic acid with or without vehicle of KA [Veh (KA) or Veh] was replaced 2 h after glutamine and glutamic acid starvation at the start of the culture. Lower panel shows data that are 12 h after the start of the culture in upper panel. Data were normalized by the values of photon count just before treatment. Normalized luciferase reporter activities of neonatal PT slices from heterozygous *TSH*β^{Luc} mice housed under L12:D12 conditions are shown. (n = 3-4, average ± SEM). White and black bars on the graphs indicate the subjective day and night on the following days after sampling, respectively. ZT12 is the start of subjective night and the culture was started at the time point.

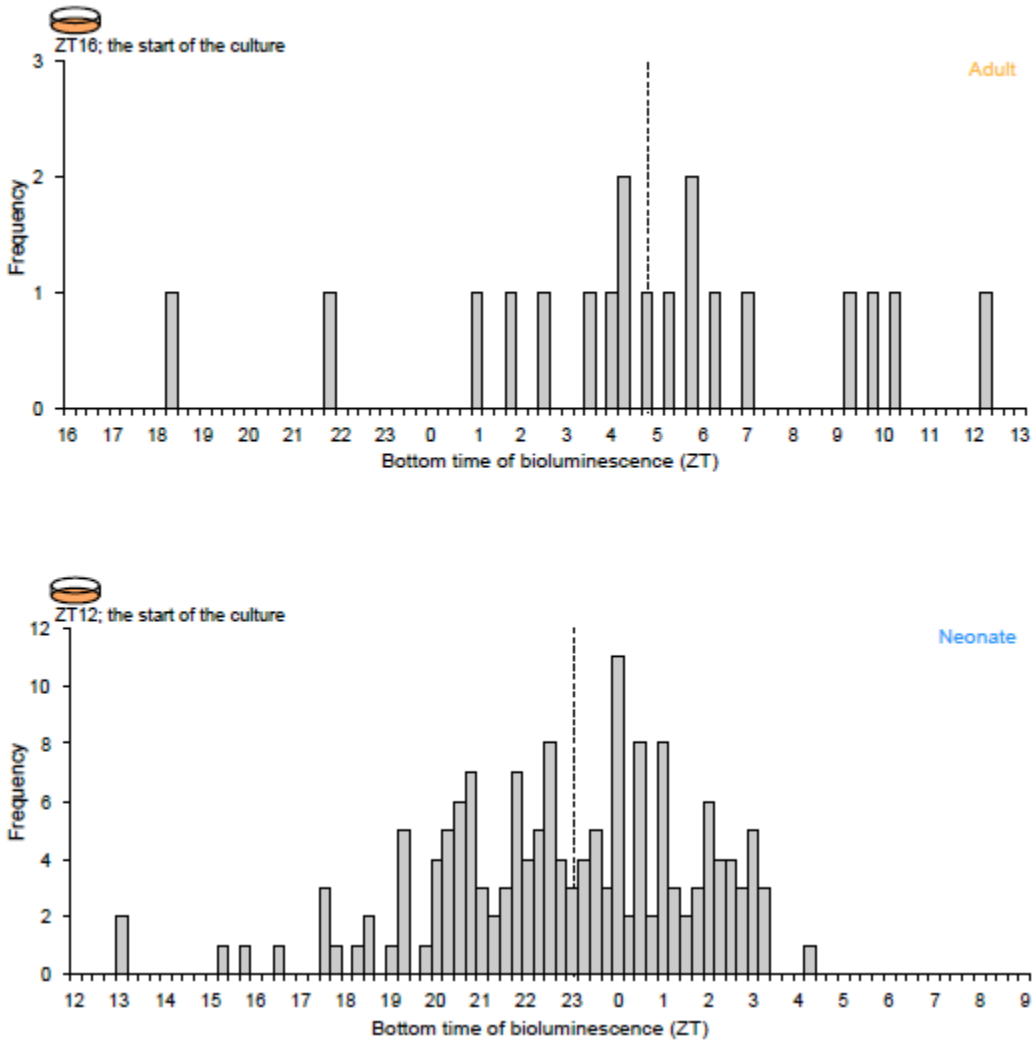

Figure 13. Histograms of the bottom time of bioluminescence of adult long-day PT samples (n = 19, upper) and neonatal PT samples (n = 157, bottom) that were treated with vehicle. The median time (ZT4.75 in adult long-day, ZT23 in neonate) was indicated as dash lines. ZT16 in upper panel and ZT12 in lower panel mean the start time of the culture.

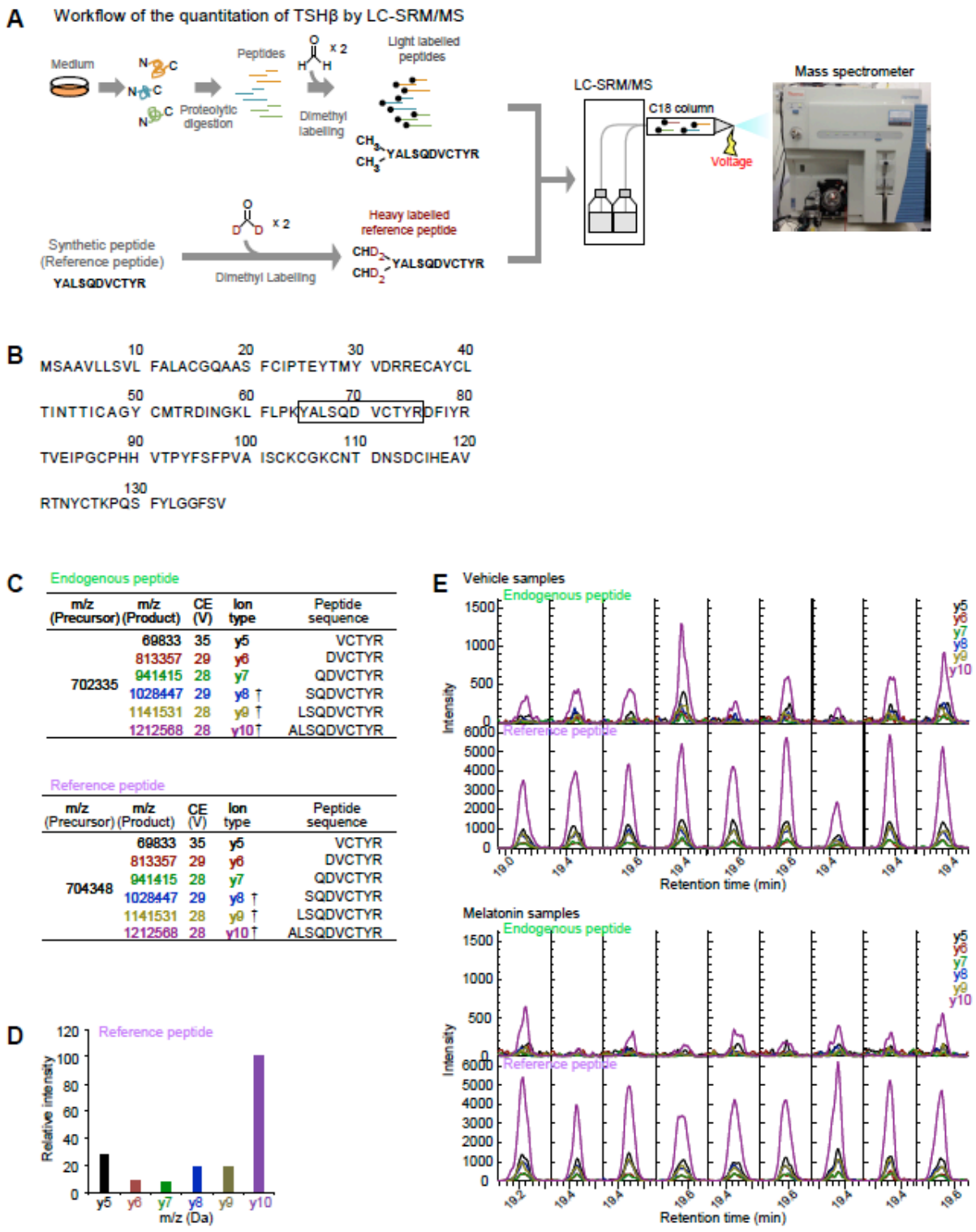

Figure 14. The chromatograms of each selected reaction monitoring (SRM) transition. (A) Experimental schema. The culture medium of the PT slices was collected and digested. The resultant digest was dimethyl labelled with formaldehyde (CH_2O). Synthetic peptide for reference was dimethyl labelled with

formaldehyde (CD_2O). Each peptide was desalted by C18 StageTips and quantified by mass spectrometry. See Experimental procedures. (B) Amino acid sequence of TSHβ. Box indicates reference peptide sequence. (C) SRM transition parameters. CE means collision energy. †; The SRM transitions were used for quantification. (D) Relative intensity of each SRM transitions of reference peptides. (E) Chromatograms of endogenous peptides from the medium (each upper column) and synthetic peptides (each bottom column) are shown. The x-axis scale is 0.05 min per division.

References

Abe, M., Herzog, E.D., Yamazaki, S., Straume, M., Tei, H., Sakaki, Y., Menaker, M. & Block, G.D. (2002) Circadian rhythms in isolated brain regions. *J Neurosci* **22**, 350-356.

Aizawa, S., Sakai, T. & Sakata, I. (2012) Glutamine and glutamic acid enhance thyroid-stimulating hormone beta subunit mRNA expression in the rat pars tuberalis. *J Endocrinol* **212**, 383-394.

Ansari, N., Agathagelidis, M., Lee, C., Korf, H.W. & von Gall, C. (2009) Differential maturation of circadian rhythms in clock gene proteins in the suprachiasmatic nucleus and the pars tuberalis during mouse ontogeny. *Eur J Neurosci* **29**, 477-489.

Atcha, Z., Cagampang, F.R., Stirland, J.A., Morris, I.D., Brooks, A.N., Ebling, F.J., Klingenspor, M. & Loudon, A.S. (2000) Leptin acts on metabolism in a photoperiod-dependent manner, but has no effect on reproductive function in the seasonally breeding Siberian hamster (Phodopus sungorus). *Endocrinology* **141**, 4128-4135.

Bünning, E. (1936) Die endogene Tagesrhythmik als Grundlage der photoperiodischen Reaktion. *Ber. Dtsch. Bot. Ges.* **54**, 590–607.

Balsalobre, A., Marcacci, L. & Schibler, U. (2000) Multiple signaling pathways elicit circadian gene expression in cultured Rat-1 fibroblasts. *Curr Biol* **10**, 1291-1294.

Beamer, W.J., Eicher, E.M., Maltais, L.J. & Southard, J.L. (1981) Inherited primary hypothyroidism in mice. *Science* **212**, 61-63.

Bockmann, J., Bockers, T.M., Winter, C., Wittkowski, W., Winterhoff, H., Deufel, T. & Kreutz, M.R. (1997) Thyrotropin expression in hypophyseal pars tuberalis-specific cells is 3,5,3'-triiodothyronine, thyrotropin-releasing hormone, and pit-1 independent. *Endocrinology* **138**, 1019-1028.

Boersema, P.J., Raijmakers, R., Lemeer, S., Mohammed, S. & Heck, A.J. (2009) Multiplex peptide stable isotope dimethyl labeling for quantitative proteomics. *Nat Protoc* **4**, 484-494.

Brydon, L., Roka, F., Petit, L., de Coppet, P., Tissot, M., Barrett, P., Morgan, P.J., Nanoff, C., Strosberg, A.D. & Jockers, R. (1999) Dual signaling of human Mel1a melatonin receptors via G(i2), G(i3), and G(q/11) proteins. *Mol Endocrinol* **13**, 2025-2038.

Cheng, M.Y., Bullock, C.M., Li, C., Lee, A.G., Bermak, J.C., Belluzzi, J., Weaver, D.R., Leslie, F.M. & Zhou, Q.Y. (2002) Prokineticin 2 transmits the behavioural circadian rhythm of the suprachiasmatic nucleus. *Nature* **417**, 405-410.

Choudhary, D., Jansson, I., Stoilov, I., Sarfarazi, M., Schenkman, JB. (2005) Expression patterns of mouse and human CYP orthologs (families 1-4) during development and in different adult tissues. *Arch Biochem Biophys* **436**, 50-61. 2005

Ciarleglio, C.M., Axley, J.C., Strauss, B.R., Gamble, K.L. & McMahon, D.G. (2011) Perinatal photoperiod imprints the circadian clock. *Nat Neurosci* **14**, 25-27.

Cordier, A.C., Denef, J.F. & Haumont, S.M. (1976) Thyroid gland in dwarf mice: a stereological study. *Cell Tissue Res* **171**, 449-457.

Dardente, H., Wyse, C.A., Birnie, M.J., Dupre, S.M., Loudon, A.S., Lincoln, G.A. & Hazlerigg, D.G. (2010) A molecular switch for photoperiod responsiveness in mammals. *Curr Biol* **20**, 2193-2198.

Dawson, A., King, V.M., Bentley, G.E. & Ball, G.F. (2001) Photoperiodic control of seasonality in birds. *J Biol Rhythms* **16**, 365-380.

Dupre, S.M., Burt, D.W., Talbot, R., Downing, A., Mouzaki, D., Waddington, D., Malpaux, B., Davis, J.R., Lincoln, G.A. & Loudon, A.S. (2008) Identification of melatonin-regulated genes in the ovine pituitary pars tuberalis, a target site for seasonal hormone control. *Endocrinology* **149**, 5527-5539.

Dupre, S.M., Miedzinska, K., Duval, C.V., Yu, L., Goodman, R.L., Lincoln, G.A., Davis, J.R., McNeilly, A.S., Burt, D.D. & Loudon, A.S. (2010) Identification of Eya3 and TAC1 as long-day signals in the sheep pituitary. *Curr Biol* **20**, 829-835.

Ebihara, S., Marks, T., Hudson, D.J. & Menaker, M. (1986) Genetic control of melatonin synthesis in the pineal gland of the mouse. *Science* **231**, 491-493.

Ebling, F.J. & Barrett, P. (2008) The regulation of seasonal changes in food intake and body weight. *J Neuroendocrinol* **20**, 827-833.

Ebling, F.J., Claypool, L.E. & Foster, D.L. (1988) Neuroendocrine responsiveness to light during the neonatal period in the sheep. *J Endocrinol* **119**, 211-218.

Ebling, F.J., Wood, R.I., Suttie, J.M., Adel, T.E. & Foster, D.L. (1989) Prenatal photoperiod influences neonatal prolactin secretion in the sheep. *Endocrinology* **125**, 384-391.

Goldman, B., Hall, V., Hollister, C., Roychoudhury, P., Tamarkin, L. & Westrom, W. (1979) Effects of melatonin on the reproductive system in intact and pinealectomized male hamster maintained under various photoperiods. *Endocrinology* **104**, 82-88.

Guilding, C., Hughes, A.T., Brown, T.M., Namvar, S. & Piggins, H.D. (2009) A riot of rhythms: neuronal and glial circadian oscillators in the mediobasal hypothalamus. *Mol Brain* **2**, 28.

Halford, S., Pires, S.S., Turton, M., Zheng, L., Gonzalez-Menendez, I., Davies, W.L., Peirson, S.N., Garcia-Fernandez, J.M., Hankins, M.W. & Foster, R.G. (2009) VA opsin-based photoreceptors in the hypothalamus of birds. *Curr Biol* **19**, 1396-1402.

Hamner, W.M. (1963) Diurnal Rhythm and Photoperiodism in Testicular Recrudescence of the House Finch. *Science* **142**, 1294-1295.

Hanon, E.A., Lincoln, G.A., Fustin, J.M., Dardente, H., Masson-Pevet, M., Morgan, P.J. & Hazlerigg, D.G. (2008) Ancestral TSH mechanism signals summer in a photoperiodic mammal. *Curr Biol* **18**, 1147-1152.

Hanon, E.A., Routledge, K., Dardente, H., Masson-Pevet, M., Morgan, P.J. & Hazlerigg, D.G. (2010) Effect of photoperiod on the thyroid-stimulating hormone neuroendocrine system in the European hamster (Cricetus cricetus). *J Neuroendocrinol* **22**, 51-55.

Harney, J.P., Scarbrough, K., Rosewell, K.L. & Wise, P.M. (1996) In vivo antisense antagonism of vasoactive intestinal peptide in the suprachiasmatic nuclei causes aging-like changes in the estradiol-induced luteinizing hormone and prolactin surges. *Endocrinology* **137**, 3696-3701.

Hoffman, R.A. & Reiter, R.J. (1965) Pineal Gland: Influence on Gonads of Male Hamsters. *Science* **148**, 1609-1611.

Ikegami, K. & Yoshimura, T. (2012) Circadian clocks and the measurement of daylength in seasonal reproduction. *Mol Cell Endocrinol* **349**, 76-81.

Ishikawa, T., Tamai, Y., Zorn, A.M., Yoshida, H., Seldin, M.F., Nishikawa, S. & Taketo, M.M. (2001) Mouse Wnt receptor gene Fzd5 is essential for yolk sac and placental angiogenesis. *Development* **128**, 25-33.

Isojima, Y., Nakajima, M., Ukai, H. *et al.* (2009) CKIepsilon/delta-dependent phosphorylation is a temperature-insensitive, period-determining process in the mammalian circadian clock. *Proc Natl Acad Sci U S A* **106**, 15744-15749.

Izumo, M., Sato, T.R., Straume, M. & Johnson, C.H. (2006) Quantitative analyses of circadian gene expression in mammalian cell cultures. *PLoS Comput Biol* **2**, e136.

Japon, M.A., Rubinstein, M. & Low, M.J. (1994) In situ hybridization analysis of anterior pituitary hormone gene expression during fetal mouse development. *J Histochem Cytochem* **42**, 1117-1125.

Johnston, J.D., Messager, S., Ebling, F.J., Williams, L.M., Barrett, P. & Hazlerigg, D.G. (2003) Gonadotrophin-releasing hormone drives melatonin receptor down-regulation in the developing pituitary gland. *Proc Natl Acad Sci U S A* **100**, 2831-2835.

Kasahara, T., Abe, K., Mekada, K., Yoshiki, A. & Kato, T. (2010) Genetic variation of melatonin productivity in laboratory mice under domestication. *Proc Natl Acad Sci U S A* **107**, 6412-6417.

Kasukawa, T., Masumoto, K.H., Nikaido, I., Nagano, M., Uno, K.D., Tsujino, K., Hanashima, C., Shigeyoshi, Y. & Ueda, H.R. (2011) Quantitative expression profile of distinct functional regions in the adult mouse brain. *PLoS One* **6**, e23228.

Kennaway, D.J., Voultsios, A., Varcoe, T.J. & Moyer, R.W. (2002) Melatonin in mice: rhythms, response to light, adrenergic stimulation, and metabolism. *Am J Physiol Regul Integr Comp Physiol* **282**, R358-365.

Kobayashi, K., Ikeda, Y., Haneda, E. & Suzuki, H. (2008) Chronic fluoxetine bidirectionally modulates potentiating effects of serotonin on the hippocampal mossy fiber synaptic transmission. *J Neurosci* **28**, 6272-6280.

Kobayashi, K., Ikeda, Y., Sakai, A., Yamasaki, N., Haneda, E., Miyakawa, T. & Suzuki, H. (2010) Reversal of hippocampal neuronal maturation by serotonergic antidepressants. *Proc Natl Acad Sci U S A* **107**, 8434-8439.

Kobayashi, K., Ikeda, Y. & Suzuki, H. (2011) Behavioral destabilization induced by the selective serotonin reuptake inhibitor fluoxetine. *Mol Brain* **4**, 12.

Kramer, A., Yang, F.C., Snodgrass, P., Li, X., Scammell, T.E., Davis, F.C. & Weitz, C.J. (2001) Regulation of daily locomotor activity and sleep by hypothalamic EGF receptor signaling. *Science* **294**, 2511-2515.

Kraves, S. & Weitz, C.J. (2006) A role for cardiotrophin-like cytokine in the circadian control of mammalian locomotor activity. *Nat Neurosci* **9**, 212-219.

Lambert, G.W., Reid, C., Kaye, D.M., Jennings, G.L. & Esler, M.D. (2002) Effect of sunlight and season on serotonin turnover in the brain. *Lancet* **360**, 1840-1842.

Lincoln, G.A., Andersson, H. & Loudon, A. (2003) Clock genes in calendar cells as the basis of annual timekeeping in mammals--a unifying hypothesis. *J Endocrinol* **179**, 1-13.

Mangmool, S. & Kurose, H. (2011) G(i/o) protein-dependent and -independent actions of Pertussis Toxin (PTX). *Toxins (Basel)* **3**, 884-899.

Marians, R.C., Ng, L., Blair, H.C., Unger, P., Graves, P.N. & Davies, T.F. (2002) Defining thyrotropin-dependent and -independent steps of thyroid hormone synthesis by using thyrotropin receptor-null mice. *Proc Natl Acad Sci U S A* **99**, 15776-15781.

Martin, L.B., Weil, Z.M. & Nelson, R.J. (2008) Seasonal changes in vertebrate immune activity: mediation by physiological trade-offs. *Philos Trans R Soc Lond B Biol Sci* **363**, 321-339.

Masuda, T., Tomita, M. & Ishihama, Y. (2008) Phase transfer surfactant-aided trypsin digestion for membrane proteome analysis. *J Proteome Res* **7**, 731-740.

Masumoto, K.H., Ukai-Tadenuma, M., Kasukawa, T., Nagano, M., Uno, K.D., Tsujino, K., Horikawa, K., Shigeyoshi, Y. & Ueda, H.R. (2010) Acute induction of Eya3 by late-night light stimulation triggers TSHbeta expression in photoperiodism. *Curr Biol* **20**, 2199-2206.

Morgan, P.J., Davidson, G., Lawson, W. & Barrett, P. (1990) Both pertussis toxin-sensitive and

insensitive g-proteins link melatonin receptor to inhibition of adenylate cyclase in the ovine pars tuberalis. *J Neuroendocrinol* **2**, 773-776.

Morgan, P.J., Lawson, W., Davidson, G. & Howell, H.E. (1989) MELATONIN INHIBITS CYCLIC AMP PRODUCTION IN CULTURED OVINE PARS TUBERALIS CELLS. *Journal of Molecular Endocrinology* **3**, R5-R8.

Morgan, P.J. & Williams, L.M. (1996) The pars tuberalis of the pituitary: a gateway for neuroendocrine output. *Rev Reprod* **1**, 153-161.

Murata, T., Furushima, K., Hirano, M., Kiyonari, H., Nakamura, M., Suda, Y. & Aizawa, S. (2004) ang is a novel gene expressed in early neuroectoderm, but its null mutant exhibits no obvious phenotype. *Gene Expr Patterns* **5**, 171-178.

Nakahara, D., Nakamura, M., Iigo, M. & Okamura, H. (2003) Bimodal circadian secretion of melatonin from the pineal gland in a living CBA mouse. *Proc Natl Acad Sci U S A* **100**, 9584-9589.

Nakane, Y., Ikegami, K., Ono, H., Yamamoto, N., Yoshida, S., Hirunagi, K., Ebihara, S., Kubo, Y. & Yoshimura, T. (2010) A mammalian neural tissue opsin (Opsin 5) is a deep brain photoreceptor in birds. *Proc Natl Acad Sci U S A* **107**, 15264-15268.

Nakane, Y., Shimmura, T., Abe, H. & Yoshimura, T. (2014) Intrinsic photosensitivity of a deep brain photoreceptor. *Curr Biol* **24**, R596-597.

Nakao, N., Ono, H., Yamamura, T. *et al.* (2008) Thyrotrophin in the pars tuberalis triggers photoperiodic response. *Nature* **452**, 317-322.

Narumi, R., Murakami, T., Kuga, T., Adachi, J., Shiromizu, T., Muraoka, S., Kume, H., Kodera, Y., Matsumoto, M., Nakayama, K., Miyamoto, Y., Ishitobi, M., Inaji, H., Kato, K. & Tomonaga, T. (2012) A Strategy for Large-Scale Phosphoproteomics and SRM-Based Validation of Human Breast Cancer Tissue Samples. *J Proteome Res* **11**, 5311-5322.

Ono, H., Hoshino, Y., Yasuo, S., Watanabe, M., Nakane, Y., Murai, A., Ebihara, S., Korf, H.W. & Yoshimura, T. (2008) Involvement of thyrotropin in photoperiodic signal transduction in mice. *Proc Natl Acad Sci U S A* **105**, 18238-18242.

Pittendrigh, C.S. & Minis, D.H. (1964) The entrainment of circadian oscillation by light and their role as photoperiodic clocks. *The American Naturalist* **98**, 261-294.

Prosser, R.A. & Gillette, M.U. (1989) The mammalian circadian clock in the suprachiasmatic nuclei is reset in vitro by cAMP. *J Neurosci* **9**, 1073-1081.

Ravault, J.P. & Ortavant, R. (1997) Light control of prolactin secretion in sheep. Evidence for photoinducible phase during rhythm. . *Ann. Biol. anim. Bioch. Biophys.* **17**, 459-473.

Revel, F.G., Masson-Pevet, M., Pevet, P., Mikkelsen, J.D. & Simonneaux, V. (2009) Melatonin controls

seasonal breeding by a network of hypothalamic targets. *Neuroendocrinology* **90**, 1-14.

Roca, A.L., Godson, C., Weaver, D.R. & Reppert, S.M. (1996) Structure, characterization, and expression of the gene encoding the mouse Mel1a melatonin receptor. *Endocrinology* **137**, 3469-3477.

Roseboom, P.H., Namboodiri, M.A., Zimonjic, D.B., Popescu, N.C., Rodriguez, I.R., Gastel, J.A. & Klein, D.C. (1998) Natural melatonin 'knockdown' in C57BL/6J mice: rare mechanism truncates serotonin N-acetyltransferase. *Brain Res Mol Brain Res* **63**, 189-197.

Rusak, B. & Morin, L.P. (1976) Testicular responses to photoperiod are blocked by lesions of the suprachiasmatic nuclei in golden hamsters. *Biol Reprod* **15**, 366-374.

Schulze-Bonhage, A. & Wittkowski, W. (1990) Age-dependent changes of ultrastructure and thyroid-stimulating hormone immunoreactivity in the pars tuberalis of the rat. *Acta Anat (Basel)* **139**, 134-140.

Shigeyoshi, Y., Taguchi, K., Yamamoto, S., Takekida, S., Yan, L., Tei, H., Moriya, T., Shibata, S., Loros, J.J., Dunlap, J.C. & Okamura, H. (1997) Light-induced resetting of a mammalian circadian clock is associated with rapid induction of the mPer1 transcript. *Cell* **91**, 1043-1053.

Shimomura, K., Lowrey, P.L., Vitaterna, M.H., Buhr, E.D., Kumar, V., Hanna, P., Omura, C., Izumo, M., Low, S.S., Barrett, R.K., LaRue, S.I., Green, C.B. & Takahashi, J.S. (2010) Genetic suppression of the circadian Clock mutation by the melatonin biosynthesis pathway. *Proc Natl Acad Sci U S A* **107**, 8399-8403.

Stetson, M.H. & Watson-Whitmyre, M. (1976) Nucleus suprachiasmaticus: the biological clock in the hamster? *Science* **191**, 197-199.

Tanaka, S., Akiyoshi, T., Mori, M., Wands, J.R. & Sugimachi, K. (1998) A novel frizzled gene identified in human esophageal carcinoma mediates APC/beta-catenin signals. *Proc Natl Acad Sci U S A* **95**, 10164-10169.

Taylor, B.A. & Rowe, L. (1987) The congenital goiter mutation is linked to the thyroglobulin gene in the mouse. *Proc Natl Acad Sci U S A* **84**, 1986-1990.

Ukai, H., Kobayashi, T.J., Nagano, M., Masumoto, K.H., Sujino, M., Kondo, T., Yagita, K., Shigeyoshi, Y. & Ueda, H.R. (2007) Melanopsin-dependent photo-perturbation reveals desynchronization underlying the singularity of mammalian circadian clocks. *Nat Cell Biol* **9**, 1327-1334.

Unfried, C., Ansari, N., Yasuo, S., Korf, H.W. & von Gall, C. (2009) Impact of melatonin and molecular clockwork components on the expression of thyrotropin beta-chain (Tshb) and the Tsh receptor in the mouse pars tuberalis. *Endocrinology* **150**, 4653-4662.

Williams, L.M., Martinoli, M.G., Titchener, L.T. & Pelletier, G. (1991) The ontogeny of central melatonin binding sites in the rat. *Endocrinology* **128**, 2083-2090.

Yagi, T., Tokunaga, T., Furuta, Y., Nada, S., Yoshida, M., Tsukada, T., Saga, Y., Takeda, N., Ikawa, Y. & Aizawa, S. (1993) A novel ES cell line, TT2, with high germline-differentiating potency. *Anal Biochem* **214**, 70-76.

Yagita, K. & Okamura, H. (2000) Forskolin induces circadian gene expression of rPer1, rPer2 and dbp in mammalian rat-1 fibroblasts. *FEBS Lett* **465**, 79-82.

Yamashita, T., Ohuchi, H., Tomonari, S., Ikeda, K., Sakai, K. & Shichida, Y. (2010) Opn5 is a UV-sensitive bistable pigment that couples with Gi subtype of G protein. *Proc Natl Acad Sci U S A* **107**, 22084-22089.

Yasuo, S., Watanabe, M., Iigo, M., Nakamura, T.J., Watanabe, T., Takagi, T., Ono, H., Ebihara, S. & Yoshimura, T. (2007) Differential response of type 2 deiodinase gene expression to photoperiod between photoperiodic Fischer 344 and nonphotoperiodic Wistar rats. *Am J Physiol Regul Integr Comp Physiol* **292**, R1315-1319.

Yasuo, S., Yoshimura, T., Ebihara, S. & Korf, H.W. (2010) Photoperiodic control of TSH-beta expression in the mammalian pars tuberalis has different impacts on the induction and suppression of the hypothalamo-hypopysial gonadal axis. *J Neuroendocrinol* **22**, 43-50.

Yellon, S.M., Fagoaga, O.R. & Nehlsen-Cannarella, S.L. (1999) Influence of photoperiod on immune cell functions in the male Siberian hamster. *Am J Physiol* **276**, R97-R102.

Yoo, S.H., Yamazaki, S., Lowrey, P.L., Shimomura, K., Ko, C.H., Buhr, E.D., Siepka, S.M., Hong, H.K., Oh, W.J., Yoo, O.J., Menaker, M. & Takahashi, J.S. (2004) PERIOD2::LUCIFERASE real-time reporting of circadian dynamics reveals persistent circadian oscillations in mouse peripheral tissues. *Proc Natl Acad Sci U S A* **101**, 5339-5346.

Yoshimura, T., Yasuo, S., Watanabe, M., Iigo, M., Yamamura, T., Hirunagi, K. & Ebihara, S. (2003) Light-induced hormone conversion of T4 to T3 regulates photoperiodic response of gonads in birds. *Nature* **426**, 178-181.

Acknowledgements

I would like to express my deepest gratitude to Prof. Hiroki R. Ueda who gave me an opportunity to start this study. His continuous suggestions greatly helped and encouraged me. I deeply appreciate Drs. Etsuo A. Susaki and Koh-hei Masumoto whose suggestions greatly contributed in this study. I would like to appreciate Mr. Yuta Shinohara and Dr. Ryohei Narumi for synthesizing peptides and performing mass spectrometry. I would like to express my gratitude to Drs. Yasufumi Shigeyoshi and Mamoru Nagano who greatly helped me with performing *in situ* hybridization and provided me with valuable discussion. I would be grateful to Dr. Qun-Yong Zhou for providing recombinant PK2 and helpful discussion and Dr. Katsunori Kobayashi for stimulating discussions and useful suggestions. I would like to thank Dr. Shigehiro Kuraku for the ABI prism 7900 equipment, Mr. Takaya Abe, Mr. Kenichi Inoue, Dr. Hiroshi Kiyonari and Dr. Kazuki Nakao for providing us *TSH*β^{Luc} mice with IVF technique. I am grateful to the Laboratory for Animal Resources and Genetic Engineering for housing the mice, Drs. Masayuki Iigo and Atsushi Wada for helpful discussions. I would also like to thank all of members of Prof. Hiroki R. Ueda's laboratory for helpful supports, critical suggestions, and fruitful discussions.